SELIN TEMI

EXPRESSION OF GENES INVOLVED IN STEROIDOGENESIS PATHWAY FROM TESTICULAR AND EPIDIDYMAL SAMPLES OF OBESE AND NON-OBESE RATS

MASTER THESIS

2024

NEAR EAST UNIVERSITY

INSTITUTE OF GRADUATE STUDIES

DEPARTMENT OF MEDICAL GENETICS

MSc PROGRAM in MEDICAL BIOLOGY AND GENETICS

EXPRESSION OF GENES INVOLVED IN STEROIDOGENESIS PATHWAY FROM TESTICULAR AND EPIDIDYMAL SAMPLES OF OBESE AND NON-OBESE RATS

M.Sc. THESIS

Selin TEMI

Nicosia

June, 2024

NEAR EAST UNIVERSITY
INSTITUTE OF GRADUATE STUDIES
DEPARTMENT OF MEDICAL GENETICS
MSc PROGRAM in MEDICAL BIOLOGY AND GENETICS

EXPRESSION OF GENES INVOLVED IN STEROIDOGENESIS PATHWAY FROM TESTICULAR AND EPIDIDYMAL SAMPLES OF OBESE AND NON-OBESE RATS

M.Sc. THESIS

Selin TEMI

Supervisor
Prof. Pınar TULAY

Nicosia
June, 2024

Approval

We certify that we have read the thesis submitted by Selin Temi titled "**EXPRESSION OF GENES INVOLVED IN STEROIDOGENESIS PATHWAY FROM TESTICULAR AND EPIDIDYMAL SAMPLES OF OBESE AND NON-OBESE RATS**" and that in our combined opinion it is fully adequate, in scope and in quality, as a thesis for the degree of Master of Sciences.

Examining Committee	Name-Surname	Signature
Head of the Committee:	Assist Prof Emrah Guler	.....
Committee Member*:	Dr. Gulten Tuncel	.....
Supervisor:	Prof. Pinar Tulay	.....

Approved by the Head of the Department

24./.06/2024

.....

Prof. Pinar Tulay

Head of the Department

Approved by the Institute of Graduate Studies

...../...../ 20...

Prof. Dr. Kemal Hüsnü Can Başer

Head of the Institute of Graduate Studies

Declaration

I hereby declare that all information, documents, analysis and results in this thesis have been collected and presented according to the academic rules and ethical guidelines of Institute of Graduate Studies, Near East University. I also declare that as required by these rules and conduct, I have fully cited and referenced information and data that are not original to this study.

Selin TEMİ

…../…../…..

Acknowledgments

I would like to express my deepest gratitude to my supervisor Prof. Dr. Pınar TULAY, for her patience and feedback throughout my research. Special thanks to both Dr. Gulten TUNCEL and Dr. Hakan AYTACOGLU for the thoughtful comments and recommendations on this research. I would also like to thank Prof. Dr. Seda Vatansever for providing us with the sample. Finally, thanks to my family for their unconditional support this academic year.

Selin Temi

Abstract

EXPRESSION OF GENES INVOLVED IN STEROIDOGENESIS PATHWAY FROM TESTICULAR AND EPIDIDYMAL SAMPLES OF OBESE AND NON-OBESE RATS

Temi Selin
M.Sc Program in Medical Biology and Genetics,
Department of Medical Genetics
June 2024, 58 pages

The World Health Organization (WHO, 2022) uses body mass index (BMI) to determine the obesity. Obese is classified as a patient with a BMI above 30>kg/m^2. Obesity is associated with some diseases such as hypertension, epigenetic alterations, type II diabetes, cardiovascular diseases, and kidney disease. Besides these disorders, obesity also contributes to hormonal dysfunction and impaired spermatogenesis which leads to hypogonadism. All of them could increase rates of male infertility. Steroidogenesis is the multi-staged process by which cholesterol is transformed into biologically active steroid hormones, which play an essential role in physiological and developmental functions. The gonads produce testosterone and estrogen and these adrenals produce mineralocorticoids and glucocorticoids.

In this study, a total of 11 rats were used to investigate the association of obesity and the expression pattern of a number of selected genes involved in the steroidogenesis pathway, i.e *Cyp11a1, Cyp17a1, Hsd3b2, Hsd17b1*. Total RNA extraction followed by cDNA synthesis was performed for each sample prior to real time polymerase chain reaction. The $2^{-\Delta\Delta Ct}$ was used to calculate the fold changes in gene expression, and -ΔCt demonstrates the quantity of cycles (Ct) of the target genes with the endogenous control. All values were normalized to the β-actin gene ACTB used as the housekeeping genes in the analysis. Although, this study showed expression of *Cyp11a1*, and *Cyp17a1*, there was no statistical significance between obese and non-obese rats of testicular samples ($p>0.05$). Similarly, both *Hsd3b2*, and *Hsd17b1* expression was shown in testicular and epididymal samples of rats with no statistical significance when comparing the epididymis of obese and control groups ($p>0.05$). Further statistical analysis including the Kolmogorov-Smirnov and Kruskal-

Wallis also showed that there was no statistical significance in the expression level of the investigated genes in different sample groups. Future research with a larger sample and various conditions will be planned.

***Key Words**:* obesity, steroidogenesis, testes, epididymis, gene expression.

Özet

EXPRESSION OF GENES INVOLVED IN STEROIDOGENESIS PATHWAY FROM TESTICULAR AND EPIDIDYMAL SAMPLES OF OBESE AND NON-OBESE RATS

Temi Selin
M.Sc, Department of Medical Genetics
June 2024, 58 pages

Dünya Sağlık Örgütü (WHO,2006) aşırı kilo ve obeziteyi vücut kitle indeksi (BMI) olarak tanımlamıştır. Obez, BMI sonucu 30>kg/m^2'nin üzerinde olan hasta olarak sınıflandırılır. Obezite, hipertansiyon, epigenetik değişiklikler, diyabet, kardiyovasküler hastalıklar ve böbrek hastalığı gibi bazı hastalıklarla ilişkilidir. Bu bozuklukların yanı sıra obezite aynı zamanda hormonal fonksiyon bozukluğuna ve hipogonadizme yol açan bozulmuş spermatogeneze de katkıda bulunur. Bunların hepsi erkek kısırlığı oranlarını artırabilir. Steroidogenez, kolesterolün fizyolojik ve gelişimsel işlevlerde önemli bir rol oynayan biyolojik olarak aktif steroid hormonlara dönüştüğü çok aşamalı bir süreçtir. Steroidogenez yolağının ilk basamağı testosteron ve östrojen üreten gonadlardadır. Bunun yanı sıra adrenaller mineralokortikoidler ve glukokortikoidler üretir.

Bu çalışmada steroidogenez genleri olan *Cyp11a1, Cyp17a1, Hsd3b2, Hsd17b1* gen ekspresyonunun sıçanların obezite ve kontrol gruplarına etkisini araştırmak amacıyla toplam 11 sıçan kullanıldı. $2^{-\Delta\Delta Ct}$, gen ifadesindeki kat değişikliklerini hesaplamak için kullanıldı ve -ΔCt, endojen kontrol ile hedef genlerin döngülerinin (Ct) miktarını gösterdi. Tüm değerler, analizde house-keeping geni olarak kullanılan β-aktin geni ACTB'ye göre normalleştirildi. Bu çalışmada sıçanların testislerindeki *Cyp11a1* ve *Cyp17a1* ekspresyonunun obez ve obez olmayan sıçanlar arasında istatistiksel olarak anlamlı olmadığı ($p>0.05$), hem *Hsd3b2* hem de *Hsd17b1* ekspresyonunun sıçanlarda testis ve epididimis, obez ve kontrol karşılaştırıldığında istatistiksel olarak anlamlı olmadığı gözlemlendi ($p>0.05$). Alınan sonuclar dogrultusunda, ileri istatistiksel çalışma olarak Kolmogorov-Smirnov ve Kruskal Wallis istatistikleri incelendi, fakat bu çalışmalarda da anlamlı bir sonuca varılamadı.

Bu çalışmada, bulgular daha geniş bir örneklem ve çeşitli koşullarla daha fazla araştırmaya ihtiyaç olduğunu göstermiştir.

***Anahtar Kelimeler**:* obez, steroidogenez, testis, epidimis, gen ifade analizleri.

Table of Contents

Approval ……..……1

Declaration ……..2

Acknowledgements …….....3

Abstract ……..4

Summary ……..6

Table of Contents. ……..8

List of Tables……..11

List of Figures…….12

List of Abbreviations……..14

CHAPTER I

Introduction…….16

Statement of the Problem ……...16

Purpose of the Study ..……..…..16

Research Questions / Hypotheses ……..16

Significance of the Study ……...17

Limitations……..17

CHAPTER II

Mammalian Gametogenesis……18

How Mammalian Oogenesis Occur?…….……18

How Mammalian Spermatogenesis Occur?……..…….19

HPG Axis-Endocrine Hormones-ROS And Obese Male……..……..21

Steroidogenesis Pathway……..……..…22

Classic Pathway…….……..…..24

Alternative – Backdoor Pathway……...……..….26

CYP11A and *StAR* Gene Deficiency……..……..……..29

HSD3B2 Gene Deficiency……32

CYP17A1 Gene Deficiency……..34

HSD17B1 Gene Deficiencies……..36

CYP19A1 Gene Deficiencies……..37

CHAPTER III

Animals……..39

Real-Time Quantitative Polymerase Chain Reaction (qRT-PCR)…….39

Gel Electrophoresis……..40

Gene expression of Cyp11a1 in testicular and epididymal samples from rat…..41

Gene expression of Cyp17 in testicular and epididymal samples from rat…..41

Gene expression of Hsd3b2 and Hsd17b1 in testicular and epididymal samples from rat……41

Statistics……42

CHAPTER IV

Result……..43

Cyp11a1 gene expression in testes……..43

Cyp17a1 gene expression in testes……..47

Hsd3b2 and Hsd17b1 gene expression in testes and epididymis…….50

CHAPTER V

Discussion……..58

CHAPTER VI

Conclusion and Recommendations ……..61

Recommendations ……...……61

Recommendations According to Findings…….……..…..61

Recommendations for Further Research ……...…....61

References…. …….63

Appendices……..67

CV……...……68

Turnitin Report……69

List of Tables

	Page
Table 1. qRT-PCR primers sequences.	40
Table 2. Ct-Values of Steroidogenesis Genes in qRT-PCR	44
Table 3. Kolmogorov-Smirnov analysis	57
Table 4. Kruskal Wallis statistical analysis	57

List of Figures

	Page
Figure 1. Classic Pathway of Steroidogenesis	26
Figure 2. Alternative/Backdoor Pathway of Steroidogenesis	28
Figure 3. Gel electrophoresis result showing the products obtained following amplification of Cyp11a1 gene	45
Figure 4. *Cyp11a1 Gene Expression Results using qRT-PCR Amplification*	46
Figure 5. Melting Curve Analysis following Cyp11a1 Gene Amplification using qRT-PCR	46
Figure 6. The Bar Chart Showing the Cyp11a1 Gene Expression Level in Rat Samples.	47
Figure 7. Gel electrophoresis result showing the products obtained following amplification of Cyp17a1 gene.	48
Figure 8. Cyp17a1 Gene Expression Results using qRT-PCR Amplification.	48
Figure 9. Melting Curve Analysis following Cyp17a1 Gene Amplification using qRT-PCR	49
Figure 10. The Bar Chart Showing the Level of Cyp17a1 Gene Expression in Rat Samples	50
Figure 11. Hsd3b2 Gene Expression Result using qRT-PCR Amplification	51
Figure 12. Melting Curve Analysis following Hsd3b2 Gene Amplification using qRT-PCR	52
Figure 13. The Bar Chart Showing the Hsd3b2 Gene Expression Level in Rat Samples	52
Figure 14. Hsd17b1 Gene Expression Result using qRT-PCR	53

Figure 15. Melting Curve Analysis following Hsd17b1 Gene Amplification using qRT-PCR. 54

Figure 16. Melting Curve Analysis following Hsd17b1 Gene Amplification using qRT-PCR. 55

Figure 17. The Bar Chart Showing the Hsd17b1 Gene Expression Level in Rat Samples 55

List of Abbreviations

17-OHPREG:	17α-hydroxypregnolone
17OH-Allo:	17-OH Alloprogrogesterone
17OHP:	17α-Hydroxyprogesterone
3β-HSD:	3β-Hydroxysteroid
BMI:	Body Mass Index
CAIS:	Complete Androgen Insensitivity Syndrome
CTR:	Normal Control Group
CYB5:	Cytochrome B5
CYP11B1/2:	11β-Hydroxylase
CYP17A1:	Cytochrome P450 enzyme17/ 17α-hydroxy pregnenolone
CYP19A1:	Aromatase Activity
CYP21A2:	21-Hydroxylase
DHEA-S:	Dehydroepiandroterone Sulfate
DOC:	11-Deoxycorticosterone
DSD:	Disorders of Sex Development
E_2:	Estrogen
ED:	Efferent Ducts
FDX1:	Ferredoxin
FDXR:	Ferredoxin Reductase
FSH:	Follicle Stimulating Hormone
GnRH:	Gonadotrophin-Releasing Hormone

GV:	Germinal Vesicles
HSD17B3:	17β-Hydroxysteroid Dehydrogenase 3
HSD3B2:	3β-Hydroxysteroid Dehydrogenase Type II
IMM:	Inner Mitochondrial Membrane
LH:	Luteinizing Stimulating Hormone
MetS:	Metabolic Syndrome
ND:	Normal Diet
OC:	Obese Control
OHE:	Obese High-Volume Exercise
OME:	Obese Moderate Volume Exercise
PCOS:	Polycystic Ovary Syndrome
PGSs:	Primordial Germ Cells
POR:	P450 Oxidoreductase
PREG/P5:	Pregnenolone
ROS:	Reactive – Oxygen Species
StAR:	Stereiodogenesis Acute Regulatory Protein
WHO:	World Health Organization
Δ5:	Delta 5

CHAPTER I

Introduction

Gametogenesis is the name given to the production of gametes which are sperm and egg cells. They have been produced from testes and ovaries, respectively (Marques et al., 2018). Germline is a tissue that produces gametes. Individual germ cells are referred to as germline cells. A germ cell which is an oogonium or spermatogonium undergoes meiosis to create haploid cells (n) that directly develop into gametes while in gametogenesis (Maine, 2013a). Meiosis is an essential part of gametogenesis (MacLennan et al., 2015a). Germ cells of both males and females need to undergo meiotic cell division to decrease the ploidy of the gametes. It is crucial for gamete generation and ploidy post-fertilization maintenance. Fertilization is the process of joining the sperm and egg (MacLennan et al., 2015a; Marques et al., 2018). The formation of the normal embryo which should be diploid cells (2n) consists of two chromosome sets, each set comes from each parent (Marques et al., 2018). If the embryo inherits only one copy of a chromosome it is called monosomy and develops into anomalies and mostly arrests before pregnancy. If an embryo inherits an additional chromosome number, it is called trisomy and is linked with severe developmental anomalies (Marques et al., 2018). The remarkable meiotic failure determined in pregnancies results from female meiosis failure while less than 5% are lead to failure during meiosis in male (Herbert et al., 2015).

The body mass index (BMI) is used by the World Health Organization (WHO, 2022) to define the obese and over-weight terminology. WHO, reported that 1 in 8 people in the world were living with obesity. Also, patients with a BMI of 25>kg/m2 are classified as overweight, while those with a BMI above 30>kg/m2 are classified as obese. Indeed, in 2022, 2.5 billion adults were classified as overweight including 890 million who were living with obesity. Obesity is associated with some diseases such as hypertension, epigenetic alterations, type II diabetes, cardiovascular diseases, and kidney disease (WHO, 2022). Besides these disorders, obesity also contributes to hormonal dysfunction and impaired spermatogenesis which leads to hypogonadism. All of them could increase rates of male infertility (Craig et al., 2017; Davidson et al., 2015; Kahn & Brannigan, 2017; Penzias et al., 2021; Raad et al., 2017). Actually, increased estrogen levels in males who are obese result from the high conversion of androgens into estrogens to the high aromatase enzyme bioavailability. Therefore, obesity is significantly considered to affect male

infertility. The WHO investigated how obesity affects sperm parameters and reproduction which had been classified as infertility based on sperm concentration, motility, and morphology. Many factors were demonstrated that could impair male fertility including genetic factors, endocrine hormone disruptors, congenital anomalies, vascular abnormalities, and anti-spermatogenic factors. Obesity is associated with low-level sperm concentration, abnormal morphology and motility and nonfunctional chromatin structure referred to as abnormal semen parameters (Shukla et al., 2014). Maturation represents tail growth, decrease of the cytoplasm and constitution of the acrosome, a membrane-circulated cap including enzymes, thought to be required for the oocyte penetration process. Moreover, nucleus condensation happens as the histones in the sperm chromosome's DNA are exchanged with protamine. The chromatin protamination leads to the disulfide bond generation and DNA's highly tight coiling which tends to preserve it from denaturation of chemical and physical agents. The completion period of the spermatogenesis cycle takes 72 days from the beginning which is the spermatogonia division until the spermatid is to be released to the epididymis (Shukla et al., 2014).

Steroidogenesis contains multiple enzymatic processes converting cholesterol into active steroid hormones, which serve a critical function in physiological and developmental functions (Flück & Pandey, 2014; Wang et al., 2017). The steroidogenesis pathway encompasses a series of enzymatic reactions occurring primarily in the gonads and glands, as well as in other tissues such as the placenta during pregnancy (Flück & Pandey, 2014; Scott et al., 2009). The first process of the steroidogenesis pathway occurs in gonads that produce testosterone and estrogen. As well as the adrenals produce mineralocorticoids and glucocorticoids (Flück & Pandey, 2014; Van, 2013). Notably, Leydig cells within the testes play a pivotal role in testosterone production, essential for male sexual development and secondary characteristics. Conversely, the adrenal glands contribute to the production of both androgen and corticosteroids, highlighting their critical role in maintaining hormonal balance. They are expressed in the specific parts of the human body (Flück & Pandey, 2014).

The study aimed to evaluate the expression profiles of selected genes involved in the steroidogenesis pathway; Cyp11a1, Cyp17a1, Hsd3b2, and Hsd17b1; in obese and non-obese rats.

CHAPTER II

Mammalian Gametogenesis

Fertilization occurs with the oocyte and sperm and the outcome is the totipotent zygote which causes all cell types of the organism (Ben Maamar et al., 2021; Tang et al., 2016). Primordial germ cells (PGCs), are precursor of germline, and are specified at pre-gastrulation epiblast stage of the embryo (Tang et al., 2016). The specification of PGCs is regulated by way of signals from extra-embryonic tissues (Ben Maamar et al., 2021). Human oocyte development starts with the differentiation of PGCs into oocyte in the fetal ovaries (MacLennan et al., 2015a).

The gonads serve as both endocrine glands and reproductive organs. They are essential for androgen production and spermatozoa for the male reproduction system. Additionally, they are important for estrogen hormone production and egg development in females (Latchoumycandane et al., 2018). In the testes and ovaries, PGCs differentiate into male pre-spermatogonia through signaling by Sertoli cell or female oogonia *via* granulosa cell signaling (Ben Maamar et al., 2021). When luteinizing hormone (LH) is released, Leydig cells generate testosterone, which, along with FSH, binds to the Sertoli cell receptor to regulate spermatogenesis. The oogonia maintain the similar gametogenesis process, leading to oogenesis, which leads to maturation of oocyte (Ben Maamar et al., 2021; Latchoumycandane et al., 2018).

Gametogenesis starts in the early embryonic development process during development and PGCs migration into the genital ridge at four-five weeks (Ben Maamar et al., 2021; Fang et al., 2022a). The PGCs migrate along with hindgut, and gonadal ridge where gonads differentiate into gametes after specification between at embryonic days 7.5 and 10.5 in mice (Ben Maamar et al., 2021). The gonads play the main role in the production, preservation and gamete formation. In most species, gametes are produced when they reach sexual maturity. When the germ cells fulfill meiosis from diploid to haploid spermatids and secondary oocyte, they develop into sperm and oocyte respectively (Maine, 2013).

How Mammalian Oogenesis Occur?

In mitotic cell division, daughter cells acquire two copies of each chromosome *via* DNA replication and chromosome segregation. In contrast in

meiosis just one copy of each chromosome is inherited, while in the process of gametogenesis, a single round of DNA replication is occurred then two successive rounds of chromosome segregation (Herbert et al., 2015). Meiosis consists of two stages which are MI and MII that result in one round of DNA replication (MacLennan et al., 2015). By mitotic proliferation, female meiosis leads to meiotic prophase I and into meiotic recombination (Herbert et al., 2015). During gestational week 8, the number of oogonia rises sharply to about 600,000 and reaches its maximum around the fifth month, totaling nearly 7 million. Meiosis starts at Prophase I which is separated into five different sub-types depending on chromosome conformation; leptotene within the prophase initiates and the chromosome begins to condense. The second stage is where zygotene synapsis begins. Next, crossing-over occurs in the pachytene stage. In the diplotene stage synapsis ends in diakinesis the prophase stage ends and the nuclear membrane disintegrates (Fang et al., 2022; Marques et al., 2018).

As mentioned above, the process of female oogenesis initiates when the embryonic PGC starts to differentiate into oogonia at the 6^{th} and 8^{th} week of gestation. As a result, oogonia are produced in huge numbers but most perish via apoptosis and only a few can survive. Oogonium undergoes asymmetric mitotic cell division that results in the next primary oocyte and another oogonium which results in oocyte differentiation (Marques et al., 2018). Human oocyte arrest in the meiotic process at prophase I diplotene stage with their bivalent chromosomes included in a huge nucleus which is a germinal vesicle (GV), enveloped by a small amount of cytoplasm. Then, mammalian oocytes arrest at the metaphase II phase (Fang et al., 2022b; Marques et al., 2018). Most oocyte development occurs at diplotene I arrest. There is an important change in the primary oocyte transcriptome. Then, dormant primordial follicle reactivation occurs. After this stage, meiosis I terminates. Secondary oocyte arrest at the metaphase II stage and ovulation is initiated. Indeed, after fertilization, metaphase II arrest-release occurs. Most of the primary follicles are sustained and re-activated for further oocyte maturation starting with puberty and until the menopause onset (Marques et al., 2018).

How Mammalian Spermatogenesis Occur?

Spermatogonia means reproducing male germ cells. Although the creation of oocytes occurs in early embryogenesis, spermatogenesis starts meiosis in the early

stages of puberty and it proceeds cellular differentiation. Spermatogonium starts to differentiate and undergo mitotic proliferation and maturation to form primary spermatocytes. Spermatogonia consists of two cell sub-types; Type A (dark cells, pale cells), and type B cells. Every primary spermatocyte proceeds through meiosis I and II, producing two secondary spermatocytes. These secondary spermatocytes go through meiosis II, resulting in four haploid cells, then differentiate into mature sperm cells (Fang et al., 2022; Maine, 2013).

Immature spermatozoa originating from the testes require transit through the epididymis to attain motility and fertilization capacity. Throughout the male germ cell maturation process within elongated and convoluted tubules, the plasma membrane of the sperm undergoes a series of sequential biochemical alterations due to delicate interactions with constituents of the extracellular milieu. The composition of this milieu undergoes variation across various segments of the epididymis and depends on precise timing and meticulous regulation of gene expression within the epididymis, which is a key characteristic of this organ. The epididymis comprises three distinct segments; the caput, the carpus, and the cauda. In rodents, an extra region known as the initial region is situated between the efferent ducts and the caput epididymis. Each specific section exhibits unique gene expression patterns associated with physiological functions crucial for various stages of sperm maturation. Recent studies, on epididymis in humans, have indicated the potential function of small noncoding RNAs, thereby bringing unexplored aspects of gene regulation within epididymis, including RNA stability and post-transcriptional regulation. The epididymis contributes significantly to the reproductive system of males, serving many key functions; first, receiving and concentrating immature sperm from the testis. Secondly, transporting and facilitating their maturation through subtle interactions with luminal secretions, and finally, storing mature sperm until they are released into the vas deference during ejaculation. Epididymis consists of a single convoluted tubule connecting the efferent ducts to the vas deference. Its extended length is nearly to be around 6 meters in humans, and depending on the species, it requires approximately 1 to 2 weeks for sperm to traverse its whole length. The site where sperm acquire their fertilizing ability within the epididymis varies across species (Belleannée et al., 2012).

HPG Axis-Endocrine Hormones-ROS And Obese Male

The HPG-axis represents the main point of the reproduction system (Craig et al., 2017). Under normal physiological situations, the hypothalamus produces and releases the gonadotrophin-releasing hormone (GnRH). The hypothalamus stimulates and generates follicle-stimulating hormone (FSH). In addition, luteinizing hormone (LH) also stimulates and is released *via* the anterior pituitary gland. FSH and LH have an important role in the testicle (Kahn & Brannigan, 2017). LH normally acts to stimulate steroidogenesis of the testosterone from the Leydig cells. Conversely, FSH is not highly required for spermatogenesis. However, it enhances the function of Sertoli cells leading to the main constituent for normal testicular function (Craig et al., 2017). It has been revealed that neohormones which consist of leptin and kisspeptin also affect this HPG-axis in studies. Moreover, it has been reported that obesity is linked to dysfunctional neohormones which act to change the endocrine axis of the male. In normal conditions, leptin is released by adipocytes increasing the level of kisspeptin from kiss neurons. It has acted to a high level of GnRH, enhancing FSH and LH secretion, besides enhancing biosynthesis of testosterone levels (Craig et al., 2017). Studies demonstrated that obesity can lead to conditions like hypogonadotropic hyperandrogenemia when the HPG axis is disrupted which results in a significant influence on fertility by decreasing testicular function sexual drive and modifying spermatogenesis (Davidson et al., 2015).

Obesity has been found to impact other endocrine hormones that change in the human body, according to several studies. These hormonal changes consist of alterations in the synthesis and regulation of insulin, inhibin B, leptin and the ratio between testosterone and estrogen, all of which negatively impact spermatogenesis (Davidson et al., 2015). Testosterone is secreted into the circulatory system which is included in insulin regulation, masculinization of brain, lipid metabolism, sexual behavior, erythropoietin stimulation, formation of male characteristics, such as hair growth, bone muscle mass regulation, and maturation of male sexual organs (Davidson et al., 2015; Raad et al., 2017). Moreover, testosterone indirectly regulates the HPG-axis action where by the free-circulating testosterone is fundamentally joined to albumin or to SHBG which is essentially synthesized in the liver. If an obese man who has excess body fat mass and hyperinsulinemia can change the SHBG generation in the liver, this condition will enhance level of free circulating testosterone for transformation into estrogen in body fat mass accumulated leading to

decreased secretion of GnRH in the hypothalamus. Most studies reported that in normal conditions, homeostasis of glucose and lipids are necessary for Leydig cell function. However, any changes in glucose levels or huge amounts of unsanitary fat consumption can arrest testosterone generation and stimulate apoptosis of Leydig cells. A previously published study showed that SHBG decreased the androgen clearance rate and arranged the entry into the target tissues. Moreover, the free testosterone is converted into estrogen (E2) in the adipose tissue *via* aromatase (Raad et al., 2017). Indeed, in males who are obese, increased levels of estrogen originate in the high-level bioavailability of aromatase enzyme (Shukla et al., 2014). Irregulated levels of sex hormones can affect significant changes in spermatogenesis and male reproduction systems. Obesity can cause aromatase overactivity that leads to influences on endocrinological features of white adipose tissue and dysregulation HPG-axis (Shukla et al., 2014).

As mentioned above, obesity can lead to chronic inflammatory diseases, and in addition to that it enhances reactive oxygen species (ROS) production that stimulate DNA integrity, damage plasma membrane in sperm, and increase scrotal temperature (Davidson et al., 2015; Kahn & Brannigan, 2017). Although ROS forms normally during cellular metabolism, an excess of it can attack nuclear and mitochondrial DNA, causing DNA fragmentation, abnormal recombination, and packaging defective. In contrast, a low concentration of ROS is essential and has a positive bioeffect on the normal functioning of the sperm cell (Kahn & Brannigan, 2017; Shukla et al., 2014). Obesity can induce ROS in the testicle and elevated ROS are linked to lowered sperm parameters and decreased testosterone synthesis (Kahn & Brannigan, 2017; Ruiz-Valderrama et al., 2022).

Steroidogenesis Pathway

Steroidogenesis is a multi-staged procedure which alters cholesterol into the last product of steroid hormone (Wang et al., 2017). Cholesterol is the steroid hormone precursor (Scott et al., 2009). All steroidogenesis hormones are derived from cholesterol which are component of lipids and proteins and are produced by the gonads, and adrenals during pregnancy in the placenta (Flück & Pandey, 2014; Scott et al., 2009). They have critical roles in regulating development and are necessary for physiological functions and to transport them into circulation (Tremblay, 2015; Van, 2013; Wang et al., 2017). The initial steps of the steroidogenesis pathway are gonads

which generate sex steroid production. On the other hand, adrenals generate mineralocorticoids and glucocorticoids (Flück & Pandey, 2014; Van, 2013).

As mentioned above, Leydig cells are essential for generating testosterone in male testis. Testosterone deficiency has several outcomes: increased fat mass, exhaustion, reduced bone density, muscularity, cognitive function, and immune response in adults. Testosterone biosynthesis can only happen in Leydig cells and directly occurs from cholesterol because usually, the adrenals can be precursors of testosterone, DHEA-S (dehydroepiandrosterone sulfate), and androstenedione (Scott et al., 2009). Luteinizing hormones are responsible for two crucial functions in the steroidogenesis of Leydig cells. One of them is the maintenance of optimal steroidogenesis enzyme levels. The other one is the delivery and mobilization of cholesterol into the mitochondria (Scott et al., 2009). However, inadequate steroidogenesis levels are linked with various pathological variants that are found in genes consisting of human adrenal and gonadal steroidogenesis. Even though they depend on their function and severity which include corticosteroid disorders, sex hormone deficiency-dependent cancers like prostate, breast, and ovarian, and all inherited autosomal recessive steroidogenesis genetic disorders (Boettcher & Flück, 2022; Tremblay, 2015). Indeed, during fetal development adrenal and gonadal steroids are essential for the forming process particularly when relating to androgen metabolism (Boettcher & Flück, 2022). One of the deficiencies that may occur during fetal development is complete androgen insensitivity syndrome (CAIS) which is complete lack of androgen receptors. It leads to the fetus growing into the phenotypically female characteristic regardless of the normal function and formation of the fetus (Scott et al., 2009).

Steroid production sites are the human adrenal cortex and gonads. All steroid hormones require enzyme cascade which are encoded via genes from cholesterol (Flück & Pandey, 2014). In males, the principal source of testosterone production from cholesterol is the testicular Leydig cells (Boettcher & Flück, 2022). Initiation step includes the transportation of cholesterol into the inner mitochondrial membrane (IMM), a process mediated by the steroidogenic acute regulatory protein (*StAR*) (Flück & Pandey, 2014). *StAR* is a molecule that a short-lived, expressed concerning tropic hormones, that delivers cholesterol from the outer to IMM and allows *CYP11A,* access to cholesterol (Scott et al., 2009). Their mechanism is called ‘de novo steroid hormone synthesis’ (Roelofs, 2016). Here, in the IMM, the first

steroidogenic enzyme reaction takes place, and cholesterol is altered into pregnenolone (Preg) catalyzed via *CYP11A1,* ferredoxin *(* FDX1) and ferredoxin reductase *(*FDXR) which is placed on the matrix side of the IMM (Flück & Pandey, 2014, 2017; Roelofs, 2016; Scott et al., 2009) and found in whole steroidogenic tissue but absent or poorly expressed in tissues of non-steroidogenic parts (Sanderson, 2006). This conversion can occur in two different pathways which are Δ5 steroid pregnenolone (P5) or Δ4 steroid progesterone (P4), both of them are intermediate, 17α-hydroxypregnenolone and DHEA, and 17α-hydroxyprogesterone, respectively (Scott et al., 2009). Each reaction needs both one molecule of NADH and O_2 (Payne & Hales, 2004). Then, it converges from the pathway of Δ5 to the Δ4 by *3β-HSD (*3β-hydroxysteroid) (Roelofs, 2016). *3β-HSD* has two isoenzymes; type 1 and type 2, which are organized in tissue specific manner. *3β-HSD* is found in tissues of both steroidogenic and non-steroidogenic types in humans. Type *2-3β-HSD* is mainly expressed in the adrenal cortex testis, and ovary which are referred to as steroidogenic tissues. On the other hand, type1-*3β-HSD* is synthesized in placenta, kidney, liver, and skin which are non-steroid tissues. Pregnenolone and progesterone act as the foundational precursors to generate all classes of steroid hormones (Sanderson, 2006). There can be differences in the steroidogenesis pathway in the mammalian species. For the human body, the classical pathway, Δ5 pathway, serves as the principal route for adrenal steroidogenesis while the Δ4 pathway is the preferred route for steroidogenesis in the testes (Roelofs, 2016).

Classic Pathway

Pregnenolone is converted to 17α-hydroxy-pregnolone (17-OHPreg) through pathway of delta 5 (Δ5) *via CYP17A1* in the classic pathway and further converted to DHEA (Figure 1) (Roelofs, 2016). The initial step of the reaction needs 17α-hydroxylase enzyme cascade activity and a pair of electron donation supported *via* P450 oxidoreductase (also known as *POR*), and the second reaction for DHEA synthesis needs *CYP17* lyase activity (P450c17) that separates 17,20 carbon bond, alter steroids of C21 to C19 catalyzed by cytochrome b5 (*CYB5*) that act as an allosteric factor and *POR* (Figure 1) (Flück & Pandey, 2014, 2017; Miller, 2017). Then, DHEA is converted into androstenedione *via HSD3B2* (also referred as 3β-hydroxysteroid dehydrogenase II / 3β HSD II) and further into testosterone or androstenedione *via* HSD17B3 enzyme activities (Boettcher & Flück, 2022; Flück

& Pandey, 2014). Testosterone can be converted into DHT, which has nearly ten-fold higher affinity for androgen receptor. This conversion is facilitated by 5α-reductase type II enzyme (SRD5A2/5α Red2), an enzyme synthesized in the genital skin and prostate (Flück & Pandey, 2014, 2017). On the contrary, in testis *via CYP19A1* few amounts of androstenedione and testosterone are turned into 17α-hydroxyprogesterone (17OHP), androstenedione, and testosterone. However, in this pathway, conversion to androstenedione is minimal. This is due to the insufficient or non-preferred activity of *CYP17-17,20 lyase* on the 17OHP-Preg substrate, as well as its poor activity on the 17OP substrate compared to OH-Preg. Additionally, the limited activity of *HSD3B2* further restricts this pathway (Boettcher & Flück, 2022; Flück & Pandey, 2014, 2017). It is possible to convert from pathway of delta-5 to delta-4 pathway (Scott et al., 2009; Tremblay, 2015). Interestingly, rodents generate T mostly via the Δ4 pathway.

The human adrenal cortex synthesizes various steroid hormones, including androgens from cholesterol. It expresses the whole enzymes required for testosterone formation in zona reticularis (Flück & Pandey, 2014, 2017). Additionally, the production of mineralocorticoids and glucocorticoids relies on the activity of specific enzymes, namely *CYP21A2* (P450c21) and *CYP11B1/2* (P450c11β, P450c11AS). Furthermore, *CYP17A1* is predominantly expressed in steroidogenic tissues, playing a critical role in androgens and glucocorticoid synthesis. The absence of *CYP17A1* expression results in mineralocorticoid production in the zona fasciculate, subsequently promoting glucocorticoid synthesis. Conversely, the presence of *CYP17* lyase activity in zona reticularis facilitates synthesis of adrenal C19 steroids, including DHEA and androstenedione. Hence genetic malformations affecting the initial step of steroidogenesis, common to adrenal cortex and gonadal tissues, may disrupt steroid hormone synthesis and impair reproductive development and function disorders and also adrenal deficiency, such as congenital adrenal hyperplasia (CAH) (Flück & Pandey, 2014). Defects of *CYP17A1* insufficiency or *HSD3B2* insufficiency not only cause androgen insufficiency, but also lead to insufficiency of estrogen and lead to the absence of pubertal growth and fertility impairment in normal females who have 46, XX karyotype (Miller, 2017).

Figure 1.

Classic Pathway of Steroidogenesis.

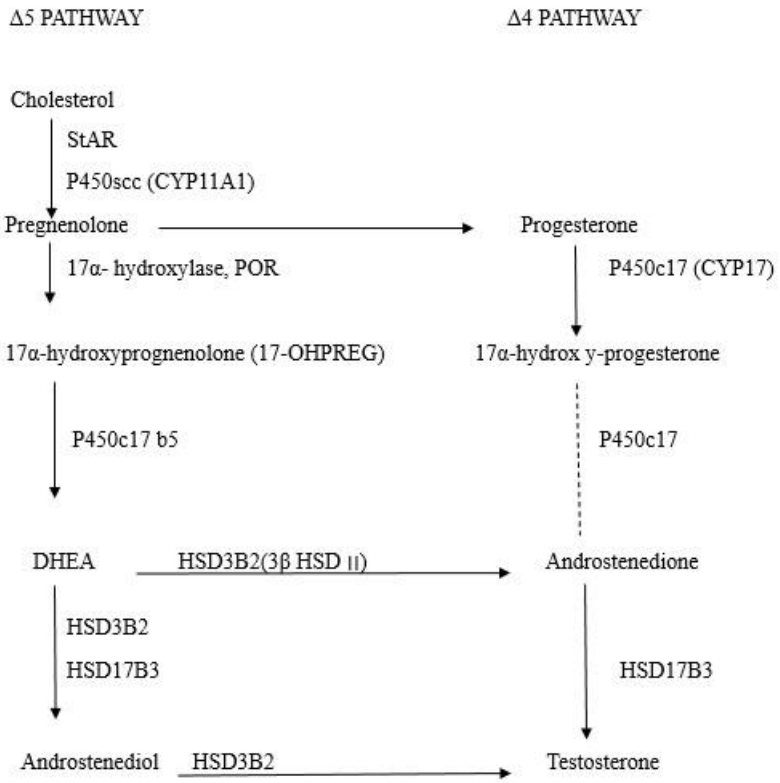

CYP11A1 converts cholesterol into pregnenolone. Pregnenolone is mediated by the Δ5 pathway into 17OHPreg and DHEA by 17α-hydroxylase, and the second reaction needs *CYB5* for DHEA synthesis. DHEA is further converted into testosterone either through the intermediacy of androstenedione or androstenediol mediated by *HSD3B2* and *HSD17B3* enzyme activities.

Alternative – Backdoor Pathway

Tamar wallaby animals are developed as unique experimental animals for various investigations, particularly because they are born at an early developmental stage before the differentiation of external genitalia occurs. Development of genitalia whilst young animals are in the pouch of the mother, provides easy access and leads to individual longitudinal development (Miller, 2017). The Tamar Wallaby studies investigated how these animals can generate DHT through an alternative pathway, known as a backdoor pathway in which 17OH-progesterone (17OHProg) is transformed into DHT without using DHEA, androstenedione, and testosterone as

intermediates, diverging from classic pathway (Flück & Pandey, 2017; Miller, 2017). In this pathway, cholesterol is first converted into Pregnenolone *via CYP11A.* Pregnenolone was further transformed into progesterone meditated by *3β-HSD.* Subsequently, progesterone is converted into 17OH-dihydroprogesterone by SRD5A1, and this intermediate is further transformed by *AKR1C2/4* into 17OH-allopregnanolone, which serves as the most favorable substrate for *CYP17A1* (17,20-lyase/POR). Androsterone was transformed into 3α-diol/androstanediol through the catalytic activity of *AKR1C3/17β-HSD*. Lastly, 3α-diol is oxidized *via* oxidative *AKR1C2/4/3α-HSD* into DHT (Boettcher & Flück, 2022; Flück & Pandey, 2017; Van, 2013). The main characteristic of the backdoor pathway, unlike the classic pathway, is that the steroid flux bypasses conventional intermediates such as DHEA, androstenedione and testosterone, and uses various enzymes such as SRD5A1 and AKRC2/4, RoDH for DHT production (Figure 2) (Flück & Pandey, 2017). There are findings for the presence of an alternative pathway in human disease and physiology. Additionally, while the backdoor pathway can originate from Δ5 pathway, it is predominantly observed in rodents. Patients with POR deficiency exhibits clinical symptoms related to both androgen excess and insufficiency (Boettcher & Flück, 2022; Flück & Pandey, 2017). Research has indicated that individuals with POR deficiency exhibit abnormally high levels of backdoor pathway intermediates, including 17OH-Allo and androsterone. In patients with first recorded *POR* mutations, a steroid profile showing 46,XX and 46,XY DSD combined with a deficiency of 21- and 17- hydroxylase, adrenal deficiency, and bone malformations (Antley-Bixley syndrome) was observed. Furthermore, a less severe phenotype resembling polycystic ovary syndrome was also identified (Flück & Pandey, 2014). Mutations in *AKR1C2* and *AKR1C4* genes show a backdoor pathway in 46, XY individuals who have mild to severe undervirilization (DSD) but there is a lack of mutations in genes when compared to the classic pathway. However, this suggests that both the classical pathway of androgen synthesis and the alternative pathway are required for sexual development in human (Flück & Pandey, 2017; Miller, 2017). The *CYP17A1* enzyme primarily catalyzes the conversion of 17OHPreg, but not 17-OHProg. It cannot utilize Preg and DHEA as substrates for 5α-reductase catalysis. The process catalyzed *via* 5α-red should occur after *CYP17A1's* action, which is the conversion of DHEA into 4-dione in humans *via 3β-HSD.* Moreover, the study demonstrated that although immature mouse testes could generate 3α-diol through

both pathways, where *CYP17A1* catalyzes process before 5α-reductase is preferred over the alternative pathway, where 5α-reductase acts before *CYP117A1* (Mahendroo et al., 2004; Van, 2013). Lastly, the studies reported that alternative backdoor genes were demonstrated to be synthesized in both tissue specific manner of a developmental phase, demonstrating that there was a shift in gene expression of 3 alternative pathway from fetal stage to adult stage in human testis (Flück & Pandey, 2017).

Figure 2.

Alternative/Backdoor Pathway of Steroidogenesis

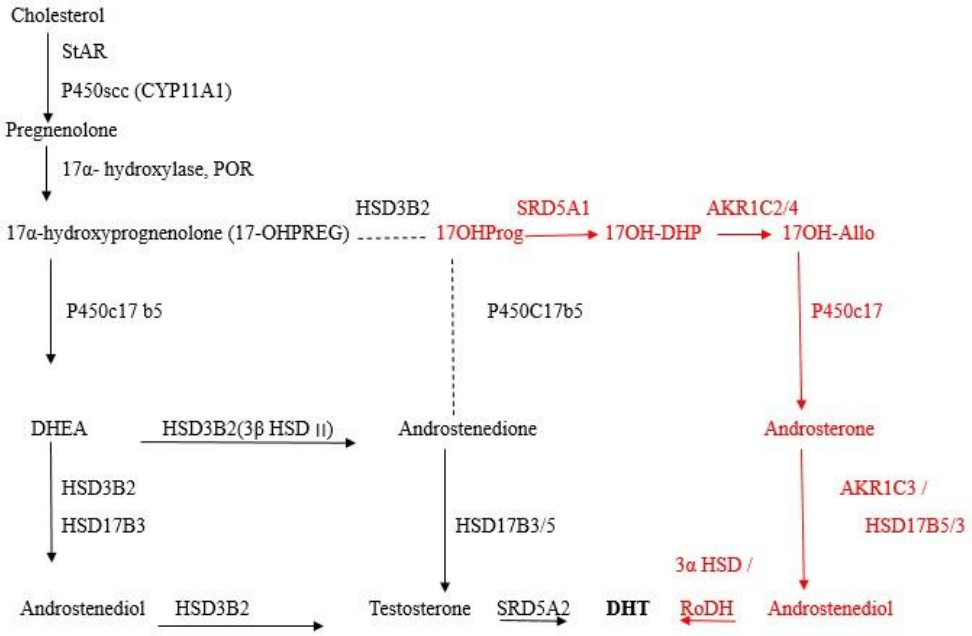

The alternative pathway is represented in red in figure 2. Cholesterol is mediated by *CYP11A1* into pregnenolone which is transformed in progesterone (PROG) by 3β-HSD. PROG is further modified by *SRD5A1* into 17OH-DHP and 17OH-Allo. Both 17OH-DHP and 17OH-Allo are then converted into androstenediol *via* the action of *AKR1C3/HSD17B5/3*. Finally, 3α-diol oxidized by oxidative *AKR1C2/4* and *AKR1C2/4 3α-HSD* into DHT (Boettcher & Flück, 2022; Flück & Pandey, 2017; Van, 2013).

CYP11A and *StAR* Gene Deficiency

CYP11A is encoded by a single gene. In 1984, Morohashi et al. isolated cDNA from the mRNA of the bovine adrenal cortex. cDNA of *CYP11A* has been cloned from humans, mice, and various other species so far. The gene structure of *CYP11A* were reported in humans and rats. The *CYP11A* is found on chromosome 15q23-24 in humans. *Cyp11a* mouse gene is found on chromosome 9 (Payne & Hales, 2004). In the initial steroidogenesis phase, the *CYP11A1* enzyme turns cholesterol to pregnenolone, which is necessary for all steroid hormone generation in adrenals, gonads, and placenta. These are steroidogenesis associated tissues (Boettcher & Flück, 2022). The main place of *CYP11A* expression has been reported as in the adrenal cortex, ovary, testis, and placenta. Indeed, *P450scc* was identified in the nervous system. *P450scc* is synthesized in whole areas; zona fasciculate, zona reticularis, and zona glomerulosa in the adrenal cortex. Within the ovary, *CYP11A* exhibits expression specifically within the theca interna and granulosa cells of the mature follicles, whereas its presence is notably absent in smaller antral follicles. In the testis, the sole expression place is the Leydig cells. During embryogenesis in mouse, the earliest identification of *Cyp11a* mRNA takes place at embryonic day 10.5 in the urogenital ridge, with remarkable expression identified within fetal testes via at embryonic day 12.5. Although P450scc mRNA persists throughout pregnancy in fetal testes, it is scarcely detected in fetal ovaries. Studies investigated steroidogenic enzyme mRNA expression in human fetal adrenal glands and gonads between 12- and 26 weeks of gestation revealed that P450scc is higher prominently expressed in adrenal glands between weeks of 20 and 21, after that by testes, with low expression in fetal ovaries. The studies demonstrated that testicular expression decreased, starting from a peak around 15 weeks to notably reduced levels by 26 weeks. After birth, both in rodents and humans, the *CYP11A* expression in the testes decreases as the fetal Leydig cell population disappears. Following the adult Leydig cell population is established around postnatal day 10 in rodents and at the beginning of puberty in humans, attaining adult expression levels by approximately day 25 postnatally in mice. *P450scc* expression in the mouse adrenal primordium was detected starting from embryonic day 11 (E11), whereas in fetal rat adrenal glands, its expression was first observed at embryonic day 12 (E12). Studies on primate fetal adrenal glands revealed that in humans, P450scc expression occurs exclusively in the fetal and transitional zones of the adrenal cortex between 14 and 22 weeks of

gestation, with expression in the definitive zone becoming apparent only after 23 weeks. During late gestation, monkey adrenal glands displayed *Cyp11a* synthesize in all three zones. After birth, the expression of adrenal *Cyp11a* is important for survival (Payne & Hales, 2004).

StAR stimulates cholesterol transport from the external membrane to the internal place, thus providing it as the required substrate for the *CYP11A1* enzyme system (FDX1 / FDXR) consisting of whole biosynthesis of steroids. Prader reported the case of a 46,XY DSD individual who passed away from an adrenal crisis in the neonatal period. Medical examination revealed extremely enlarged adrenal glands with signs of fatty infiltration. These clinical observations prompted Prader to name this condition as lipoid congenital adrenal hyperplasia (LCAH) (Flück & Pandey, 2014, 2017). Nevertheless, the identification of *StAR* gene as the basic genetic anomaly of LCAH, along with an understanding of the disease mechanism, only occurred after many years. Infants with significant *StAR* mutations referred to as classic lipoid CAH, typically exhibit adrenal deficiency shortly postnatal stage or infancy, and affected 46,XY infants showed female-appearing external genitalia (Flück & Pandey, 2017). During fetal development, the adrenal glands primarily produce DHEA, and its absence leads to low estriol levels in pregnant females. While they also produce small amounts of other steroids, the absence of these hormones does not affect the fetus's survival until birth. However, towards the final stage of gestation, there is a transition to the adult adrenal cortex, which is responsible for producing mineralocorticoids and glucocorticoids necessary for life. The lack of these hormones can lead to potentially fatal adrenal crises in the first months of life (Boettcher & Flück, 2022). Milder form mutations of *StAR*, which maintain partial activity, lead to non-classic LCAH and may show delayed-onset primary adrenal deficiency exclusively from age 4 to adulthood, except influencing male sexual development. The mechanisms of disease are identified by Knudson's two-hit hypothesis model (Flück & Pandey, 2017). The first hit leads to the loss of *StAR* activity needed to transfer cholesterol into the mitochondria of the steroid-producing cell (Flück & Pandey, 2014). However, since approximately 10% of cholesterol import takes place independently of the *StAR* gene, a second hit is required to express a significant phenotype. The second hit involves the destruction of steroidogenic cells due to the deposition of cholesterol and cholesterol esters. Consistent with this model the Leydig cells in the testes, responsible for early

androgen production during fetal development, are susceptible to early damage, leading to 46,XY DSD. Conversely, the ovaries, which remain inactive in steroidogenesis until puberty, may only exhibit susceptibility to *StAR* insufficiency after puberty occurs. Consequently, affected females may initially undergo normal pubertal development and menstruation, until a second hit strikes (Flück & Pandey, 2017).

Human *CYP11A1* mutations present with clinical features that closely resemble those of *StAR* mutations. These mutations can occur in two forms; classic, characterized by severe mutations, and nonclassic, marked by partial loss of enzyme activity. Unlike *StAR* variants, which typically result in adrenal enlargement in imaging studies, this characteristic is not detectable in *P450scc* insufficiency. In general, *StAR* deficiency is an extremely rare condition, predominantly observed in the population of Japanese, with approximately 1/300 individuals carrying the p.Q258X mutation. Conversely, founder effects in other populations may account for certain clusters. As a result, non-classic forms of LCAH resulting from *StAR* mutations have been inconsistently analyzed in larger groups of individuals studied for uncommon forms of primary adrenal deficiency, with rates reaching 30% in Japan and 11% in Turkey, respectively (Boettcher & Flück, 2022). Patients who have classic forms of *StAR* or *CYP11A1* insufficiency exhibit an overall low generation of whole steroids which are mineralocorticoids, glucocorticoids, and sex steroids in their serum or urine steroid profiles (Flück & Pandey, 2017).

Rahali et al. investigated metabolic syndrome effects on rats' spermatogenesis and steroidogenesis pathways. The study involved 16 rats and was divided into 2 groups; a CTR which represents the normal control group and a MetS represents a metabolic syndrome group with eight rats in each group. They showed that MetS led to a reduction in testicular weight and gonad somatic index against the control group. Sperm analysis from the cauda epididymis indicated that the MetS group's sperm concentration was markedly lower compared to that of the control group. The MetS group exhibited a notably higher incidence of abnormalities in both sperm head and tail morphology in comparison to the control group. Additionally, a significant decline in plasma testosterone levels was recorded in MetS rats compared to controls ($p<.05$). Indeed, considerable decline in mRNA expression of both *Cyp11a, Cyp17a1, 17Hsdb* ($p<0.05$) was shown in the testis tissues of MetS rats against the control group (Rahali et al., 2023).

Yi et al. investigated the testicular leptin and JAK-STAT pathway role in biosynthesis of testosterone. They selected male C57bl/6I mice and randomly separated them into normal diet (ND) and high-fat diet (HFD) groups. They were further separated into three groups; obese control (OC), obese-moderate volume exercise (OME), and obese-high volume exercise (OHE) groups, after 10 weeks. The investigation focus on the effects of exercise on hormone levels in obese mice. Serum leptin and E2 levels were significantly enhanced, while serum testosterone levels and the T/E2 ratio markedly reduced in obese mouse. After exercise, there was a markedly reduction in serum leptin and E2, and an increase in serum testosterone and T/E2 ratio. Compared to normal control group, mice in OC group exhibited a marked decline in both sperm count and motility ($p<0.01$). In contrast, OME group showed a significant improvement in these parameters when compared to the OC group ($p<0.01$, $p<0.05$).The OME group demonstrated significantly greater sperm count and motility compared to OC population. However, OHE population did not demonstrate a statically significant difference from OC population, and its sperm parameters remained considerably lower than those observed in the OME population. In OC experimental group, a significant decrease in mRNA expression levels of SF-1, StAR, and CYP11A1 was detected in comparison to the NC experimental group ($p<0.05$, $p<0.01$, $p<0.05$). In OHE category, mRNA expression levels of the genes downregulated by a high-fat diet were significantly increased compared to those in OC group (each $p<0.01$). However, the difference between OHE and OC groups was not statistically significant ($p>0.05$). Furthermore, when compared to NC group, OC group showed a markedly reduced in protein synthesis of CYP11A1, SF-1, and StAR (each $p<0.01$). Protein expression was a significant reversal in the OME group compared to OC group (each $p<0.01$), whereas OHE group did not show a statically significant difference ($p>0.05$) (Yi et al., 2017).

HSD3B2 Gene Deficiencies

In the adrenals and gonads, the *HSD3B2* gene encodes 3β - hydroxysteroid dehydrogenase II enzyme, which transforms steroids of delta - 5 steroids to delta - 4. To better understand the clinical and biochemical features of *HSD3B2* insufficiency, it is essential to recognize the presence of the *HSD3B1* gene which encodes a type 1 enzyme with similar activities. This gene is synthesized in placenta, liver, and peripheral tissues (Boettcher & Flück, 2022). Severe deficiency of *HSD3B2* leads to

insufficiency in mineralocorticoids, glucocorticoids, and (partially) androgens, resulting in undervirilization and virilization in 46,XY, and 46,XX patients, respectively (Flück & Pandey, 2014, 2017). Classical adrenal steroidogenesis was affected in whole pathways of steroid biosynthesis due to the absence of *HSD3B2* enzyme activity. Nevertheless, the clinical range was wide; in severe cases, individuals may experience significant salt-wasting or non-salt-wasting adrenal deficiency and disorders of sex development (DSD) at birth followed by abnormal pubertal development. Less severe cases might present with late-onset symptoms such as premature puberty pubarche during childhood or a phenotype resembling of polycystic ovary syndrome (PCOS) during puberty (Boettcher & Flück, 2022).This is attributed to the existence of two functional *HSD3B* genes in humans, which produce enzymes exhibiting comparable activity levels (Flück & Pandey, 2014, 2017). However, in *HSD3B* insufficiency, active enzyme *HSD3B1* can transform circulating androgen precursors released from adrenal or gonads into the increased active androgens in the peripheral tissues, thus elucidating for the virilization observed in 46,XX females. Similarly, because of the functioning of *HSD3B1*, infants affected by severe *HSD3B2* deficiency might be identified through newborn screening for 21-hydroxylase deficiency. This is due to the elevated levels of 17OHP, which result from the peripheral conversion of the significantly increased levels of 17OHPreg (Flück & Pandey, 2014). In general, 3-hydroxysteroid dehydrogenases (3-HSDs) transform steroids of delta 5 into delta 4 steroids. Therefore, elevated ratios of delta 5/delta 4 are indicative of *HSD3B2* insufficiency and serve as its diagnostic hallmark (Flück & Pandey, 2014).

Boettcher et al., have examined numerous variants of *HSD3B2*, showing an adequately satisfactory association between genotype and phenotype concerning adrenal salt-wasting characteristics, but they have reported that there was no association with the severity of 46,XY DSD sex disorders. Furthermore, no pathogenic mutations were detected in the *HSD3B1* gene (Boettcher & Flück, 2022). *HSD3B2* deficiency, a condition characterized by impaired steroid biosynthesis, presents with a distinct steroid profile. However, while this profile is often an indicative disorder, the gene of *HSD3B2* genetic screening is crucial to verify the diagnosis (Flück & Pandey, 2017).

Wagner et.al. reported that diet-induced obesity has a profound impact on various aspects of male reproductive health. Both short and long-term exposure to a

high-fat diet caused considerably high body weight and fat percentage, accompanied by a raised in adipocyte size and a decline in absolute testis weight. Estradiol and leptin levels in serum were elevated in obese rats, while levels of testosterone remained unaffected. However, LH levels in serum screening were decreasing in older rats compared to younger ones. Longer-term exposure to HFD resulted in decreased testicular testosterone levels and a decline in the amount of Leydig cells. Furthermore, synthesis of steroidogenic genes in the testis was dysregulated in response to obesity, with short-term obesity leading to upregulation and long-term obesity causing downregulation. Obesity is linked with chronic inflammation, indicated by elevated levels of TNFα linked also with enhanced numbers of testicular macrophages, which may contribute to the suppression of testicular steroidogenesis noticed in long-term obesity. These findings highlight the complex and diverse effects of diet-induced obesity on male reproductive function (Wagner et al., 2016).

CYP17A1 Gene Deficiencies

CYP17 deficiency has two types, and both impact androgen biosynthesis and lead to 46, XY DSD, and gonadal deficiency. The first type which is the most common involves the absence of both 17α-hydroxylase and *CYP17A* activities, whereas second form involves the failure of *CYP17A* activity which is observed solely in a few patients to date, and leads to androgen biosynthesis only. In severe cases of 17-hydroxylase insufficiency, only the mineralocorticoid synthesis pathway of steroidogenesis remains functional. Inhibition of *P45017A* enzyme leads to increased levels of 11-deoxycorticosterone and corticosterone, which in turn suppresses aldosterone and renin, resulting in hypertension and hypokalemic alkalosis in patients. Despite elevated ACTH levels, patients generally do not experience adrenal insufficiency due to the glucocorticoid activity of corticosterone. Therefore, typical steroid profile of a combined *CYP17* deficiency is characterized by high levels of 11-Deoxycorticosterone (DOC) but limited cortisol and androgens (Flück & Pandey, 2014). Despite this, these patients only have moderate glucocorticoid insufficiency, as the absence of *CYP17A1* leads to an excess production of corticosterone, which processes glucocorticoid activity. Furthermore, patients commonly exhibit hypertension with decreased renin levels, sodium retention, and hypokalemic alkalosis, all resulting from excessive production of 11-Deoxycorticosterone (Boettcher & Flück, 2022). Patients with 46,XY clinical

presentation as a result of *CYP17* insufficiency differ from apparently female to undervirilization male, characterized by the lack of Wolff structures, Mullerian structures, and intraabdominal or undescended testes. Pubertal development is absent, consisting of inguinal growth or axillary hair, and gynecomastia occurs just in incomplete insufficiency cases (Flück & Pandey, 2014). To date, over 100 variants have been documented in the *CYP17A1* gene. The majority of pathogenic mutations affecting *CYP17A1* suppress enzyme activities and are responsible for approximately 1% of whole cases of CAH. *CYP17A1* deficiency appears to be particularly prevalent in Brazil, where the presence of two repeating variants which are p.W406R and p.R362C suggests a founder impact. The complete functionality of lyase activity depends on the presence of *POR* and *CYB5.* Isolated cases of *CYP17A1* deficiency were associated with exceedingly rare missense variation placed in E305, R347, and R358 of the CYP17A protein. This process is required for androgen generation in both classic and alternative pathways (Flück & Pandey, 2017). These variations disrupt the interaction of enzymes with *POR* and notably *CYB5A* (Boettcher & Flück, 2022).

Culty et.al. investigated steroidogenesis related gene expression in murine male germ cells. They conducted a series of experiments to investigate various aspects of germ cell biology and gene expression patterns in mice and rats at different postnatal ages. They showed that *Stard10, Hmgcr,* and *Hsd17b12* were significantly highly synthesized in pachytene spermatocyte and round spermatids. On the other hand, *Stard6, Tspo, Cyp17a1, Hsd17b13,* and *Vdac1* showed higher expression in pachytene spermatocytes, while *Hsd17B4, Acbd1, Stard7, Cyp17A1,* and *Slc25A/Ant1* were more abundant in spermatogonia. In addition, the study compared the synthesis of selected genes in germ cells compared to the Leydig cells using quantitative PCR. Leydig cells exhibited significantly higher expression of *Tspo, Cyp11a1, Hsd3b2, Stard1,* and *Acbd1* compared to germ cells. Moreover, they examined protein expression of these genes in testis and sperm of adults. The findings demonstrated that CYP11A1 protein is significantly synthesized in Leydig cells and pachytene spermatocytes, while CYP17 protein is mainly observed in sperm and Leydig cells. *Hsd17b* is only identified in Leydig cells. They also analyzed the differential synthesis of genes in rat testicular germ cells across various age groups, particularly during the initial phases of development. The expression levels of *Hsd3b1* and *Cyp11a* genes were significantly altered during the transition

from gonocytes to spermatogonia. Notably, minimal expression of *Cyp17a1* was observed in rat germ cells, similar to the limited presence in mouse spermatogonia. *Cyp19a1* also exhibited minimal synthesis in gonocytes and spermatogonia of rats, aligning with findings in undifferentiated mouse spermatogonia. The comparison also highlighted expression pattern differences of certain genes between rat and mouse germ cells, indicating species-specific variations in spermatogenesis (Culty et al., 2015).

HSD17B1 Gene Deficiencies

Human 17β-hydroxysteroid dehydrogenases *(17βHSDs*) have at least 17 isoforms, some of which function primarily as reductases, while others act as oxidases, performing various physiological roles. Similar to *3HSDs, 17HSDs* are also vital for steroidogenesis, serving a crucial function in production of active gonadal steroid hormones like estradiol and testosterone. The *17HSD*s are necessary for the steroidogenesis pathway. *17HSDs f*acilitate the last stage in the biosynthesis of testosterone, the gonadal steroid hormone. Moreover, *17HSDs* do not contribute to the biosynthesis of adrenal steroids. The first of the *17HSD*/ketosteroid reductase to be identified and studied was initially isolated and characterized from the placenta in human by Jarabak et. al. Subsequently, it was cloned from a human placental library and later detected in the ovary and mammary gland (Jarabak, 1962). Human *HSD17B1* exhibits substrate specificity toward estrogens, while the rodent enzyme demonstrates versatility in utilizing both estrogens and androgens. NADPH is the optimal cofactor for converting estrone into estradiol. Notably, human *HSD17B1* displays a 100-fold higher affinity for C18 substrates compared to C19 substrates. While *HSD17B1* human mainly facilitates transformation of estrone into estradiol, *17Hsd1* in mouse and rat also effectively changes androstenedione into testosterone. *HSD17B1* gene is found on chromosome 17q11-q21 in human and is responsible for encoding a protein consisting of 327 amino acids. On the other hand, mouse gene which is *mHsd17b1* is found on chromosome 11 and encodes a protein compromising 344 amino acids. Interestingly, the human *17HSDB1* gene is placed adjacent to *HSD17BP1*, which is considered a putative pseudogene. The studies demonstrated that the mouse *17Hsd1* inhibits an overall identity of 63% with its human counterpart, while the most notable distinctions between the mouse and human type-1 enzymes lie within amino acid residues 197 to 230 and in the carboxy

terminus of these enzymes. The expression of *17HSD1* is notably abundant within the developing follicles in granulosa cells, as well as in the human placenta. Immunoreactive HSD17B1 protein was conclusively identified within the syncytiotrophoblast of the human placenta, along with human ovary in granulosa cells (Payne & Hales, 2004).

Mutations in humans have only been identified in *HSD17B3* gene, resulting in 46,XY disorders of sex development resulting from 17-ketosteroid reductase/*17HSD3* deficiency. *17HSD3* is specifically synthesized in the testes, where it converts androstenedione into testosterone, DHEA into androstenediol, androstanedione into DHT, and androsterone into androstanediol, respectively. Consequently, *17HSD3* insufficiency is a male-specific disorder, often resulting in a blind vaginal pouch. Testes are commonly situated in the pubic region, accompanied by the absence of Mullerian structures and the presence of Wolffian structures. Patients who are raised as females are virilized during puberty due to excess *HSD17B* enzymes which convert testicular androstenedione into testosterone in the periphery. Diagnosis typically involves observing a reduced ratio of testosterone to androstenedione, either in basal conditions or following hCG stimulation (Flück & Pandey, 2014).

CYP19A1 Gene Deficiencies

P450 aromatase, encoded by *CYP19A1*, plays a crucial role in synthesizing estrogen from androgen precursors. Its expression is observed in various tissues, consisting of the ovaries, testes, placenta, brain, breast, adipose tissue, and bone osteoblasts. *CYP19A1* is active during fetal life in both males and females. In cases where the fetus has a CYP19A1 deficiency, mothers may experience progressive virilization during pregnancy. This results from the fetus's inability to aromatize androgens from the fetal adrenal glands in the placenta, leading to decreased estriol levels. Consequently, increased androgen levels in utero cause 46,XX DSD at birth, resulting in different levels of virilization of the external genitalia. During the early childhood period, boys typically show the absence of symptoms of aromatase insufficiency, while females can present abdominal symptoms followed by a disrupted HPG axis leading to ovarian cysts. At puberty, estrogen deficiency causes hypogonadotropic hypogonadism in females, resulting in failure or partial progression of spontaneous pubertal development and primary amenorrhea. Women

may experience acne and hirsutism due to varying degrees of androgen excess. Delayed bone age is common because estrogen plays a significant role in the maturation of epiphyseal and closure in both male and females, and reduced bone mineral density may occur in later stages of life. There is a detrimental effect on glucose homeostasis and lipid profile in adults. Aromatase deficiency is a rare autosomal recessive disorder, results from *CYP19A1* mutations or mutations in *POR*. In the approximately 50 cases observed, a wide spectrum of *CYP19A1* mutations were determined, and the correlation between genotype and phenotype appears uncertain (Boettcher & Flück, 2022).

Lambard et.al. mentioned that the quantity of P450arom transcripts are detected in pachytene spermatocytes, in round spermatids, and in testicular spermatozoa. When they examined *Cyp19a1* expression in different stages of germ cells in adult male rats. The study found that aromatase transcript levels were higher in pachytene spermatocytes compared to round spermatids and testicular spermatozoa. Inversely, the activity of aromatase is extra intense in haploid germ cells, particularly elongated spermatids, compared to younger germ cells. The study has demonstrated that aromatase expression was observed in spermatogonia and preleptotene spermatocytes. However, in purified myoid cells, RT-PCR did not detect any aromatase transcripts, although fibronectin, a marker of peritubular cells, was present. Comparison of P450arom mRNA levels across germ cell populations revealed a three-fold higher expression in pachytene spermatocytes compared to spermatogonia or preleptotene spermatogonia. Overall, the gene is existing in the whole germ cell stages studied with higher expression observed during meiotic stages. The researchers investigated the expression of *CYP19A1* in immature germ cells and ejaculated spermatozoa from male. They observed that the *CYP19A1* was present in both immature germ cells and ejaculated sample, with a higher abundance in spermatozoa including cytoplasmic droplets. They also characterized the *CYP191A1* protein and observed variations in its molecular weight, possibly resulting from glycosylation levels. Additionally, they found that the amount of *P450arom* transcripts and aromatase activity were higher in motile spermatozoa exposed to an aromatase inhibitor (Lambard et al., 2005).

CHAPTER III
Materials And Methods

Animals

The project was approved by the Ethics Committee for Animal Experiments in agreement with the current guidelines for animal experimentation at the University of Manisa Celal Bayar (16/04/2020/77.637.435). All rat animal samples were taken from the University of Manisa Celal Bayer, Department of Histology and Embryology. In this study, a total of 11 rats, except for the *Hsd3b2* gene expression experiment were used. Four groups were established by the research team in University of Manisa Celal Bayer, Department of Histology and Embryology, i.e; Group 1; epididymis control group (EK), group 2; epididymis obesity group (EO), group 3; testis control group (TK), group 4; testis obesity group (TO). RNA extraction and cDNA synthesis were also performed in the University of Manisa Celal Bayer, Department of Histology and Embryology.

Real-Time Quantitative Polymerase Chain Reaction (qRT- PCR)

For qRT-PCR, sense and anti-sense primers were designed using Ensemble Primer3 tool program, for rat cytochrome P450 family 11 subfamily a1 *(Cyp11a1/P450scc)*, cytochrome P450 Family 17 *(Cyp17*), cytochrome P450 family 19 *(Cyp19)*, hydroxysteroid -17-beta dehydrogenase 1 *(Hsd17b1/17βhsd1),* hydroxysteroid-3-beta dehydrogenase 2 *(Hsd3b2/3β-Hsd)* (Table 1). To prevent inappropriate amplification of residual genomic DNA, exon-exon spanning primers were designed. Additionally, a BLAST analysis was performed to ensure that the primer pairs specifically matched the sequence of interest. The stock concentration was 100µM for each primer. All primers were diluted at a concentration of 1:10 to preare a working stock. For each sample, an amplification reaction was applied using quantitative real-time PCR (Table 2) with a thermocycler Himedia Insta Q96 (Himedia, Germany) and SYBR Green mix (MG-SYBR-01-400, Hibrigen, TR). The polymerase-activation program of 5 min at 95℃, followed by 40 cycles of 95℃ for 30s and 58℃ for 30s, 72℃ for 40s were performed that was followed by a gel electrophoresis to detect the correct product size and any possible formation of primer dimers. Ct values were obtained from the software directly. The $2^{-\Delta\Delta Ct}$ was used to calculate the fold changes in gene expression, and -ΔCt demonstrates the

quantity of cycles (Ct) of the target genes with the endogenous control. All values were normalized to the *β-actin gene* (*Actb*) which was used as the housekeeping gene in the analysis.

Table. 1

qRT-PCR primers sequences.

Genes Amplified	**Oligo Name**	**Base Sequence at 5´-3´**	**T_m°C**
Cyp11a1	CYP11A1rat_F	CATCAAGAACTTCGTGCCCC	59
Cyp11a1	CYP11A1rat_R	TGGAACATCTGGTAGACGGC	59
Cyp17	CYP17rat_F	ACTCAAAGCCTCTTGTCGGA	57
Cyp17	CYP17rat_R	AAGATAGGCGTGGACAGGTC	59
Cyp19	CYP19rat_F	TGTGGATGGGGATTGGAAGT	57
Cyp19	CYP19rat_R	ACAGGCTCGGGTTGTTGTTA	57
Hsd17b1	Hsd17b1rat_F	CCAXATTGCGGGATCTGAAC	59
Hsd17b1	Hsd17b1rat_R	ATCCAGTACAGCACCCACAG	59
Hsd3b2	Hsd3b2rat_F	AGGGACAAGCATCAAGGTGA	57
Hsd3b2	Hsd3b2rat_R	AGATGAAGGCTGGCACACTA	57

Gel Electrophoresis

In this study, %2 agarose gel electrophoresis was prepared. First, the required amount of agarose was calculated using 2 grams per 100 ml of Tris-acetate EDTA (TAE) electrophoresis buffer. To prepare the TAE buffer, dissolve 242 grams of Tris Base in a small amount of dH2O. Then, add 57.1 ml of Glacial Acetic Acid, followed by 100 ml of 0.5M EDTA. Add dH2O to bring the total volume to 1 liter. Autoclave the solution at 120°C for 15 minutes to sterilize. The resulting solution is a 50X TAE buffer, which should be diluted to a 1X concentration before use in the experiment. To prepare the Ethidium Bromide solution, weight out 10 mg of EtBr powder and dissolve it in 1 ml of dH2O. The agarose solution was allowed to cool and ethidium bromide, a DNA stain was added. Finally, the cooled agarose was poured into the gel casting tray and left to set at room temperature for about 30 minutes.

After adding 3µl of loading buffer and 8µl each sample of *Cyp11a1, Cyp17a1, Hsd3b1,* and *Hsd17b1* into the wells, 110V was applied for about 30 minutes. The bands were then visualized under a UV transilluminator.

Gene Expression of *Cyp11a1* in Testicular and Epididymal Samples From Rat

Gradient PCR at 57-58-59℃ was performed for *Cyp11a1* PCR optimization. The products were run on %2 gel electrophoresis. The expression analysis of *CYP11A1* was optimized with the RT-PCR conditions of 5µl SYBR Green, 0.3 µM forward primer, 0.3 µM reverse primer, 2µl cDNA, and 2.4 µl deionized water for the negative control. The polymerase chain activation program was performed for 5 minutes at 95℃, 40 cycles of 30s at 95℃, 30s at 58℃, and 40s at 72℃. Also, a melting curve was performed for 15s at 95℃, 1 min at 60℃, 15s at 95℃ and a 20s holding step.

Gene Expression of *Cyp17* in Testicular and Epididymal Samples From Rat

Gradient PCR was performed for *Cyp17* gene at 57-58-59℃ followed by gel electrophoresis during PCR optimization. The expression analysis of *Cyp17* was optimized using RT-PCR with 5µl SYBR Green, 0.5 µM forward primer, 0.5 µM reverse primer, 2µl cDNA, and 2µl deionized water for negative control. The polymerase chain program was performed for 5 minutes at 95℃, 40s cycles of 30s at 95℃, 30s at 55℃, 40s at 72℃ and 5 min at 72℃. Also, a melting curve was performed for 15s at 95℃, 1 min at 60℃, 15s at 95℃ and a 20s holding step.

Gene Expression of *Hsd3b2* and *Hsd17b1* in Testicular and Epididymal Samples From Rat

The real time PCR was optimized for *Hsd3b2* and *Hsd17b1* with 5µl SYBR Green, 0.5 µM forward primer, 0.5 µM reverse primer, 3µl cDNA, and 1µl $MgCl_2$. The polymerase chain activation program was performed for *Hsd3b2* and *Hsd17b1* for 5 minutes at 95℃, 40 cycles of 30s at 95℃, 30s at 55℃, 40s at 72℃ and 5min at 72℃. Also, a melting curve was performed for 15s at 95℃, 1 min at 60℃, 15s at 95℃ and and a 20s holding step.

Statistics

Data were reported as means ± standard error of the mean (SEM). The student's T-test was applied to analyze the potential difference in the expression levels of genes among different group of samples using Graph Pad Prism software. A value of $p>0.05$ was considered as statistically non-significant. Further statistical analysis was also performed using Kolmogorov- Smirnov test (Table 3).

CHAPTER IV

Results

RNA extraction and cDNA synthesis were performed at Manisa Celal Bayar University, Department of Embryology and Histology. These processes were performed successfully and real-time PCR analysis to evaluate the level of gene expression was performed. A total of 11 samples were obtained from obese rats and non-obese rats. Three samples (EO1, EO2, and EO3) were taken from the epididymis of obese rats, and two samples (TO1 and TO2) were taken from the testis of obese rats. Three samples (EK1, EK2, and EK3) were taken from the epididymal samples of the non-obese rats, and three samples (TK1, TK2, and TK3) were taken from the testicular samples of non-obese rats. The study investigated the steroidogenesis-associated gene expression level, *Cyp11a1, Cyp17a1, Hsd3b2,* and *Hsd17b1*, and their relation to obesity.

Cyp11a1 Gene Expression in Testes

As mentioned above, to obtain the optimized real time PCR protocol to amplify *Cyp11a1* gene, gradient PCR was used. A clear band following gel electrophoresis at approximately 237 bp was obtained for the samples tested confirming the successful amplification of the *Cyp11a1* gene (Figure 3). The gene expression pattern for *Cyp11a1* were investigated using the optimized qRT-PCR protocol as described in Chapter III (Figure 4) and followed by the melting curve analysis (Figure 5). The Ct-values obtained for each sample of *Cyp11a1* are given below (Table 2). *Cyp11a1* was not expressed in the epididymal samples obtained from obese of rats (Figure 5). The investigation demonstrated that *Cyp11a1* was expressed in the testes of obese and control groups of rats. However, there was no significant difference in the *Cyp11a1* expression level of the samples obtained from the testes in the obese group compared to the control group ($p>0.05$) (Figure 6).

Table 2.

Ct-Values Of Steroidogenesis Genes In qRT-PCR.

Steriogenesis Genes / **Samples**	**EO1**	**EO2**	**EO3**	**EK1**	**EK2**	**EK3**	**TO1**	**TO2**	**TK1**	**TK2**	**TK3**	**NEGATIVE**
Cyp11a1	--	30.9	--	31.8	30.5	27.8	27.1	27.6	27.0	24.7	25.1	27.5
Cyp17	28.1	27.0	27.6	27.6	27.1	27.4	26.0	26.1	26.5	24.2	25.5	25.8
Cyp19	--	--	--	--	--	--	--	--	--	--	--	--
Hsd3b2	29.6	29.6	29.7	29.5	28.7	30.7	27.2	18.8	21.0	19.7	26.2	27.1
Hsd17b1	27.0	27.2	26.8	27.3	26.5	27.7	26.5	14.6	22.0	21.3	25.5	24.2

Figure 3.

Gel electrophoresis result showing the products obtained following amplification of Cyp11a1 gene

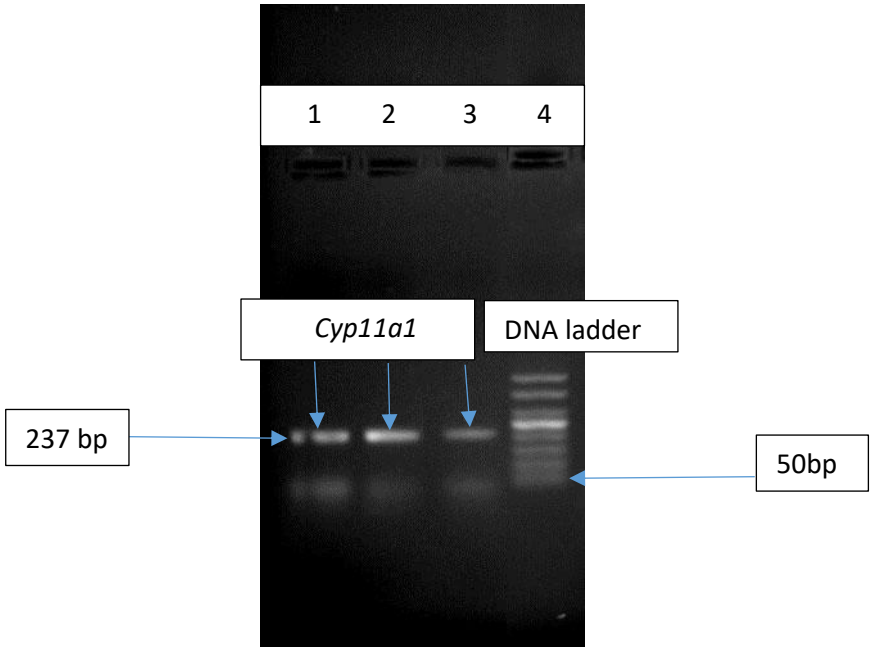

Note. Each blue arrow shows the amplified products representing the *Cyp11a1* with PCR conditions of annealing temperatures at 57℃, 58℃, 59℃, respectively (Left to right lanes 1, 2 and 3). DNA ladder is 50 bp (Lane 4). The expected product size for the *Cyp11a1* application was 237 bp.

Figure 4.

Cyp11a1 Gene Expression Results using qRT-PCR Amplification

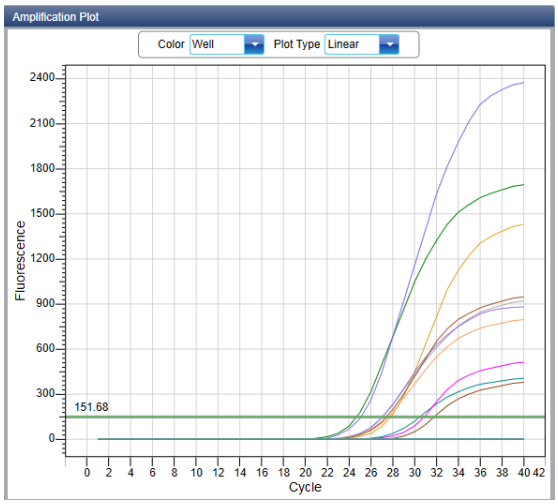

Cyp11a1 did not show any amplification in EO1 and EO3 samples, respectively. The curve colors are as follows; EO2; pink, EK1; brown, EK2; blue, EK3; yellow, TO1; purple, TO2; orange, TK1; grey, TK2; green, TK3; purple, Negative Control; brown.

Figure 5.

Melting Curve Analysis following Cyp11a1 Gene Amplification using qRT-PCR

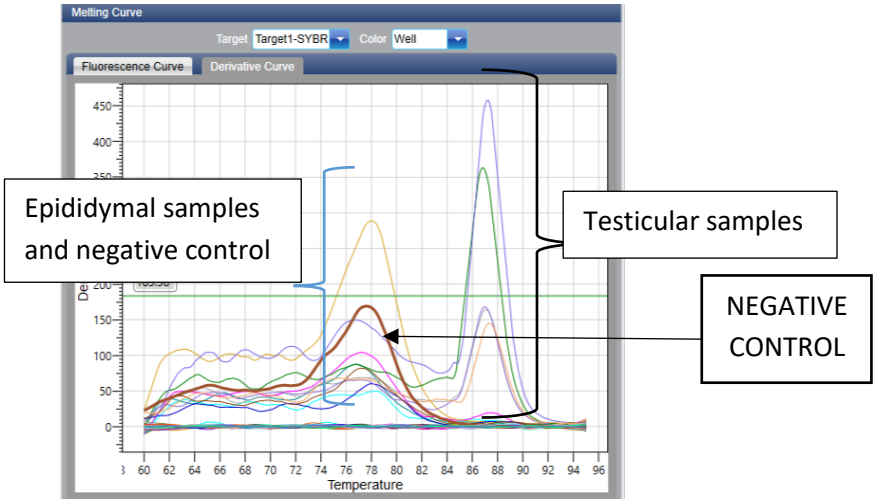

The black arrow represents the negative control. The black brace represents the testicular samples. The blue brace represents the epididymal samples. The melting curve result showed that there was a different Tm point between the negative control (primer dimer) and the amplified product obtained from testicular samples, therefore, the *Cyp11a1* gene was expressed in the testis of obese and control groups of rats. The *Cyp11a1* gene was not expressed in the epididymal samples of obese

groups of rats. The melting curve analysis showed product of the epididymal samples from obese and control groups of rats had the same peaks as negative control. The figure also showed that there was the same Tm point between the negative control (primer dimer) and amplified product obtained from epididymal samples of rats, therefore, it was assumed that the product corresponds to primer dimers.

Figure 6.
The Bar Chart Showing the *Cyp11a1 Gene Expression Level in Rat Samples.*

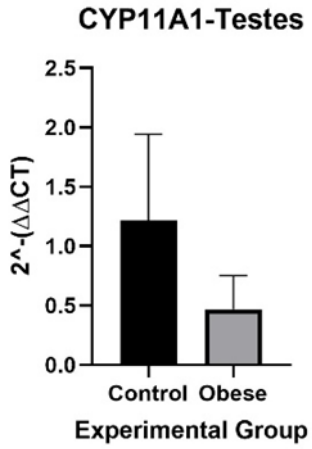

The *Cyp11a1* gene expression showed no statistically significant difference between the control and obese group of rats in the testes ($p>0.05$)

Cyp17a1 Gene Expression in Testes

The amplification of the *Cyp17a1* gene was investigated by real time PCR as described in Chapter III (Figures 7 and 8). Melting curve analysis was also performed following the real time PCR analysis (Figure 9). The Ct-values obtained for each sample of *Cyp17a1* are given above (Table 2). *Cyp17a1* was not expressed in the epididymis of the obese and non-obese rats, respectively. Indeed, *Cyp17a1* was expressed in the testes of rats in both groups. However, *Cyp17a1* expression level of samples obtained from the testes was not significant in the obese group compared to the control group ($p>0.05$) (Figure 10).

Figure 7.

Gel electrophoresis result showing the products obtained following amplification of Cyp17a1 gene.

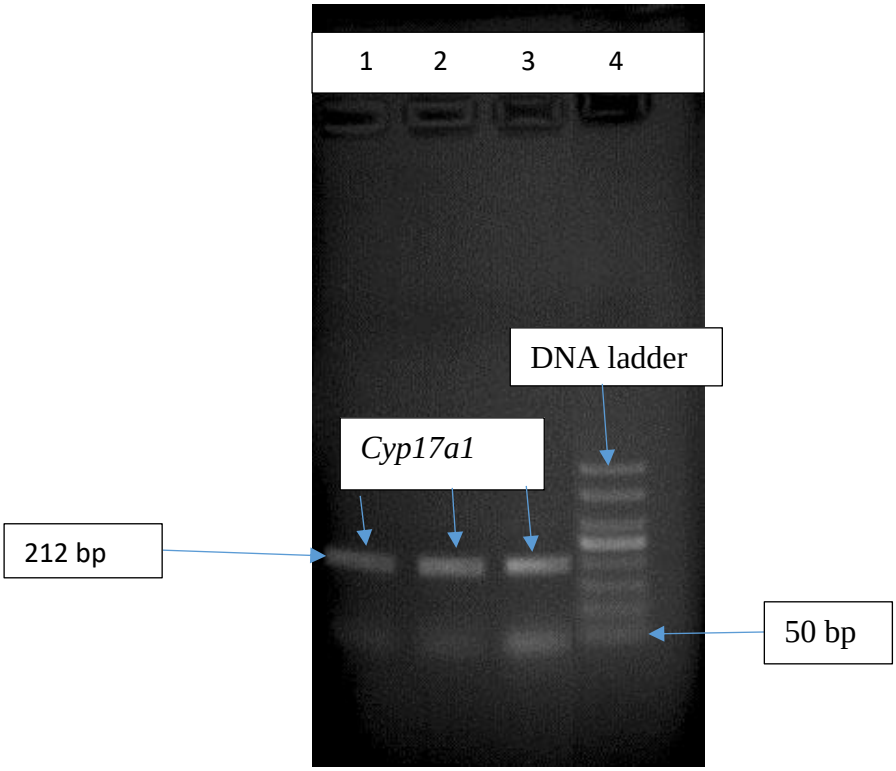

Note. Each blue arrow shows the amplified products representing the *Cyp17a1* with PCR conditions of annealing temperatures at 54-55-56℃, respectively (Left to right lanes 1,2 and 3). DNA ladder is 50 bp (Lane 4). The expected product size for the *Cyp17a1* application was 215 bp.

Figure 8.

Cyp17a1 Gene Expression Results using qRT-PCR Amplification.

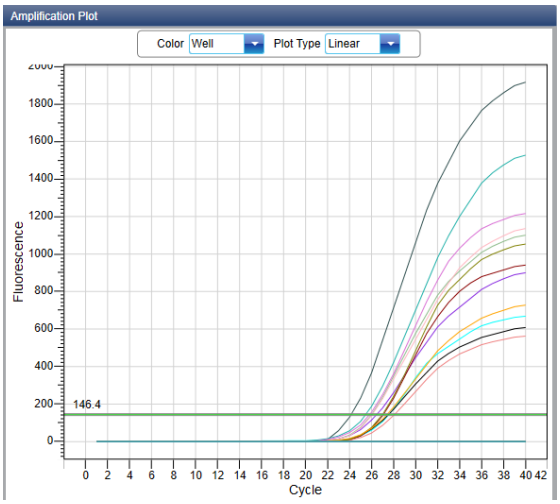

Note. The amplification curve colors for *CYP17A1* are as follows: EO1; pink, EO2; green, EO3; black, EK1; blue, EK2; red, EK3; black, TO1; light green, TO2; pink, TK1; purple, TK2; dark grey, TK3; blue, Negative Control; pink.

Figure 9.

Melting Curve Analysis following Cyp17a1 Gene Amplification using qRT-PCR

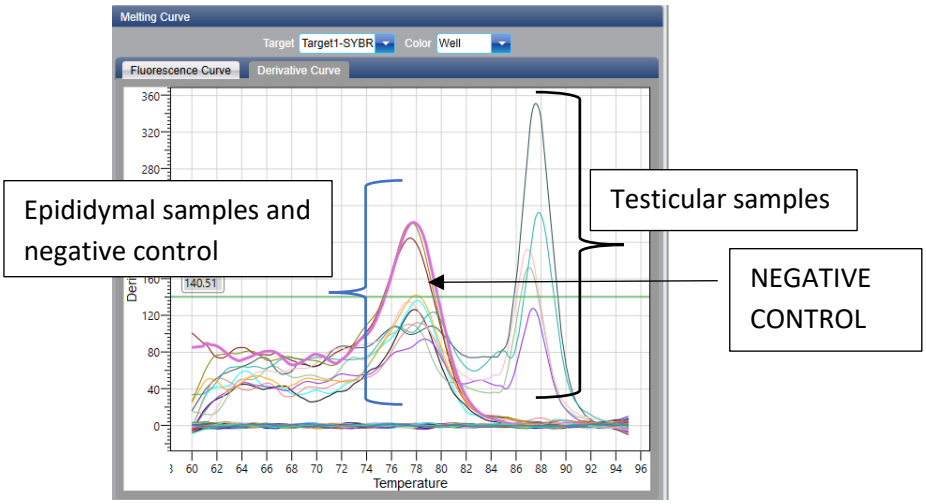

Note. A black arrow represents the negative control. The black right brace includes the testicular samples. The blue brace includes epididymal samples and negative control. The *Cyp17a1* gene is expressed in the testes of obese and control groups of rats. The melting curve result showed that there was a different Tm point between the negative control (negative control) and the amplified product obtained from testicular samples of the obese and control groups of rats. The *Cyp17a1* gene is not expressed in the epididymal samples of obese and control groups of rats. The melting curve analysis showed that the amplified product obtained from epididymis of both obese and control groups of rats appeared at the same peaks as the negative control. The figure also showed that the Tm value was the same in both the negative control (primer dimer) and epididymal sample of rats, indicating that there was primer dimers were present, and that no amplification was observed in the epididymal sample.

Figure 10.

The Bar Chart Showing the Level of Cyp17a1 Gene Expression in Rat Samples

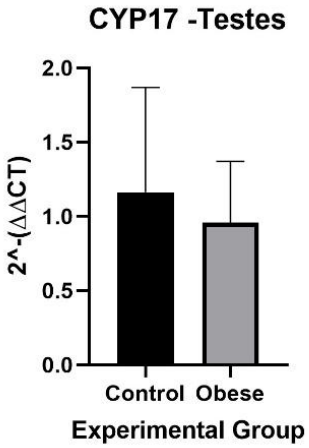

The *Cyp17a1* gene expression showed no statistically significant difference between the control and obese group of rats in the testes ($p>0.05$)

***Hsd3b2* and *Hsd17b1* gene expression in testes and epididymis.**

As described in Chapter III (Figure 11), the amplification of the *Hsd3b2* and *Hsd17b1* genes was investigated by real-time PCR. The level of the *Hsd3b2* gene expression pattern was investigated *via* qRT-PCR (Figure 12) and followed by the melting curve analysis (Figure 13). The Ct-values are given above (Table 2) The TO2 sample was excluded from the *Hsd3b2* analysis due to a failed PCR. This study demonstrated that *Hsd3b2* gene expression is present in both testicular and epididymal samples obtained from obese and control groups of rats. The expression levels in epididymal samples did not differ significantly between control and obese rats ($p>0.05$) (Figure 14-A). Similarly, no significant differences were found in the testicular samples between control and obese rats ($p>0.05$) (Figure 14-B). Additionally, when comparing the expression levels in epididymal and testicular samples from control and obese rats, no significant differences were detected ($p>0.05$) (Figure 14-C). The comparison between epididymal and testicular samples within the obese group also showed no significant differences ($p>0.005$) (Figure14-D), as well as between the control group samples ($p>0.005$) (Figure 14-E).

The level of the *Hs17ab1* gene expression pattern was investigated by qRT-PCR (Figure 15) followed by the melting curve analysis (Figure 16). The Ct-values are given above (Table 2). This study also demonstrated the presence of *Hsd17b1* gene expression in both testicular and epididymal samples obtained from obese and

control groups of rats. No significant differences in the expression levels were observed between the epididymal samples of control and obese rats ($p>0.05$) (Figure 17-A). Similarly, no significant differences were found in the testicular samples between control and obese rats ($p>0.05$) (Figure 17-B). Moreover, when comparing the expression levels in epididymal and testicular samples from control and obese rats, no significant differences were detected ($p>0.05$) (Figure 17-C). The comparison between epididymal and testicular samples within the obese group also showed no significant differences ($p>0.005$) (Figure17-D), as well as between the control group samples ($p>0.005$) (Figure 17-E).

Figure 11.

Gel electrophoresis result showing the products obtained following amplification of Hsd3b2 and Hsd17b1 genes.

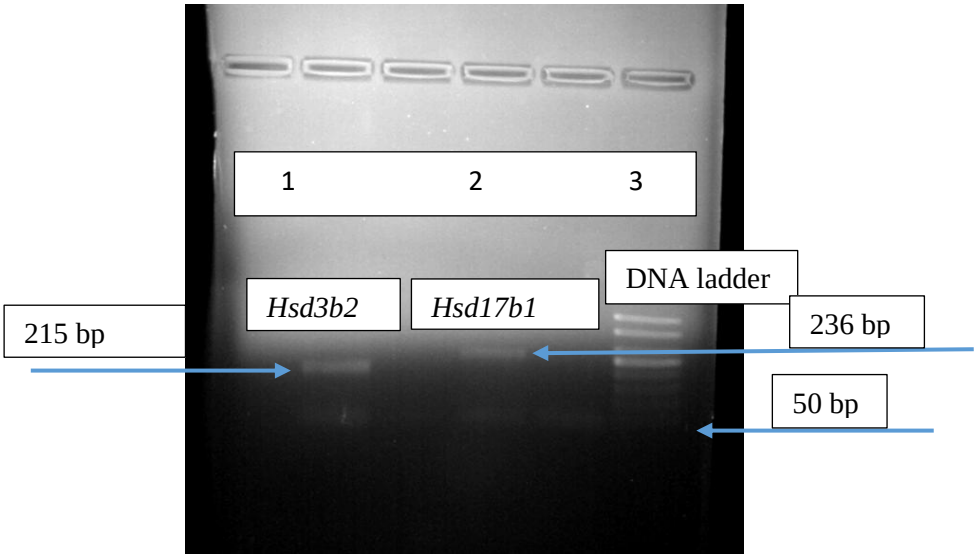

Note. Each blue arrow shows the amplified products representing the *Hsd3b2* and *Hsd17b1* with PCR conditions of annealing temperature at 56°C (Left to right lanes, 1 and 2). The DNA ladder is 50 bp (Lane 3). The expected product size for the *Hsd3b2* application was 215 bp and for the *Hsd17b1* application was 236 bp, respectively.

Figure 12.

Hsd3b2 Gene Expression Result using qRT-PCR Amplification

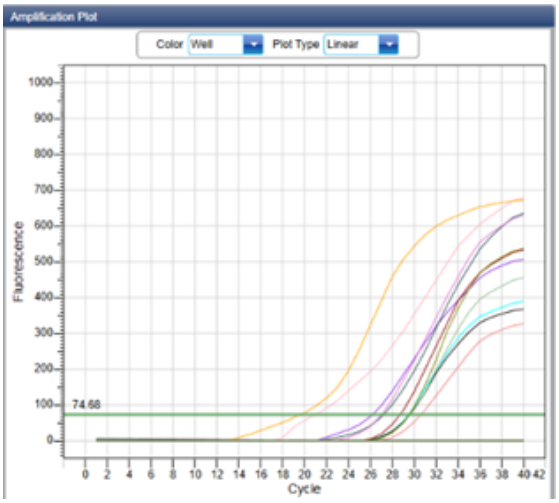

Note. The amplification curve colors for *Hsd3b2* are as follows; EO1; sap green, EO2; black, EO3; green, EK1; blue, EK2; red, EK3; pink, TO1; dark grey, TO2; amplification failure, TK1; pink, TK2; yellow, TK3; purple, Negative control; pink.

Figure 13.

Melting Curve Analysis following Hsd3b2 Gene Amplification using qRT-PCR.

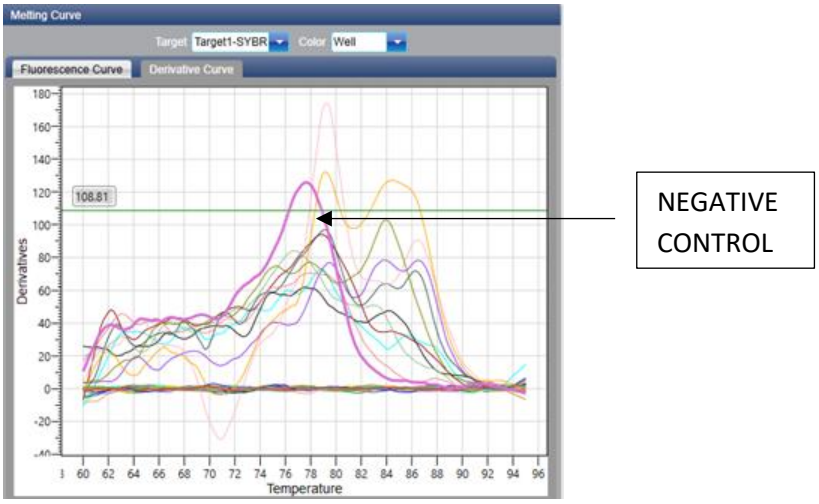

Note. A black arrow represents the negative control. The melting curve analysis showed that there was a different T_m point between the negative control (primer dimer) and amplified product obtained from the both epididymal and testicular samples of obese and control groups of rats.

Figure 14.

The Bar Chart Showing the Hsd3b2 Gene Expression Level in Rat Samples

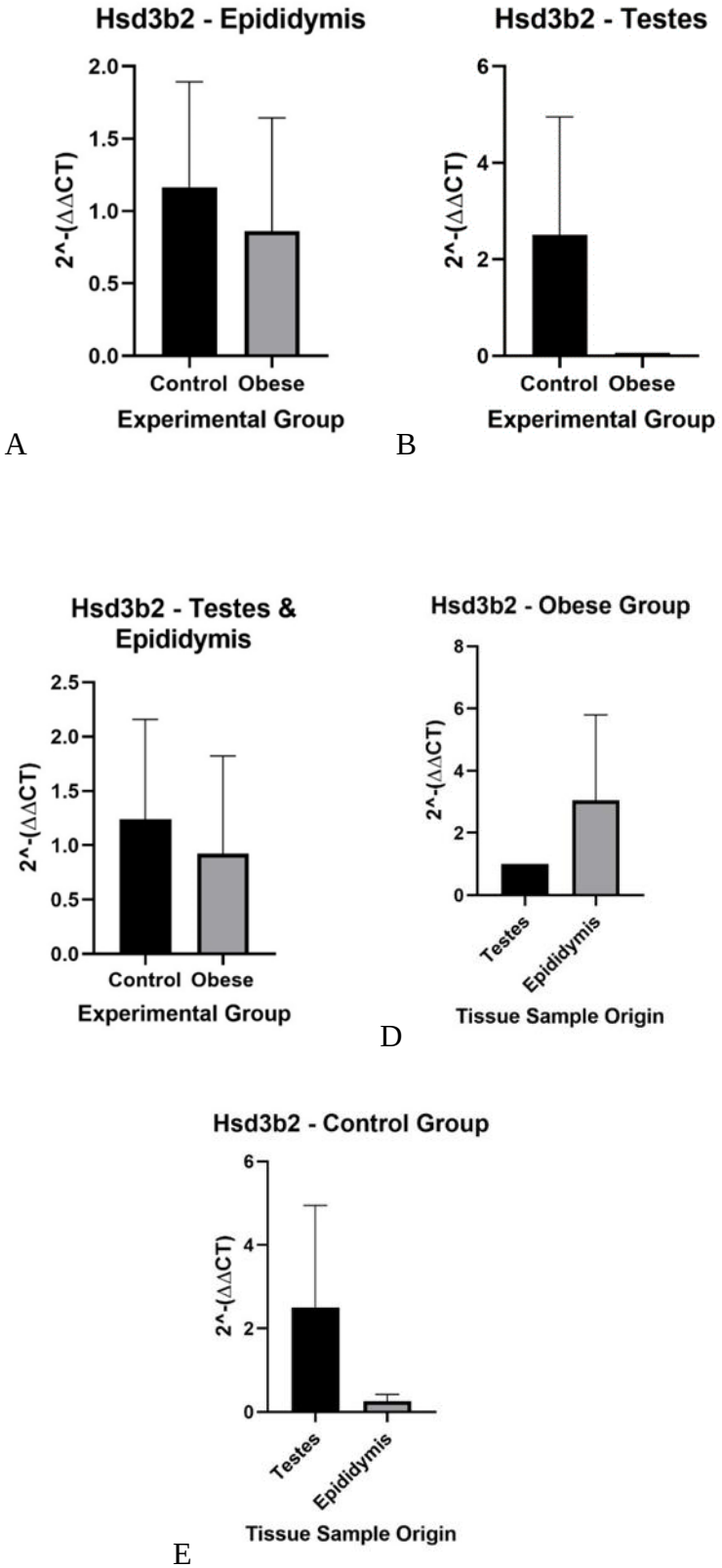

Note. A- The level of *Hsd3b2* gene expression was investigated in rat epididymal samples obtained from control and obese rats ($p>0.05$). B- The level of *Hsd3b2* gene expression was compared in rat testicular samples obtained from control and obese rats ($p>0.05$) C- The level of *Hsd3b2* gene expression was compared in rat epididymal and testicular samples obtained from control and obese rats ($p>0.05$) D- The level of *Hsd3b2* gene expression was compared in rat epididymal and testicular samples obtained from obese rats ($p>0.05$) E- The level of *Hsd3b2* gene expression was compared in rat epididymal and testicular samples obtained from control rat ($p>0.05$)

Figure 15.

Hsd17b1 Gene Expression Result using qRT-PCR.

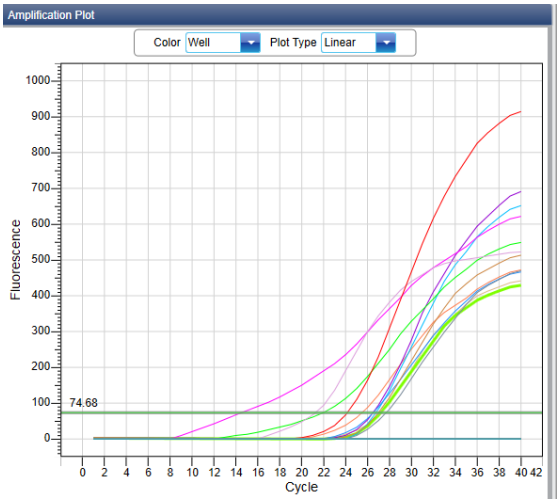

Note. The amplification curve colors for *Hsd17b1* are as follows; EO1; yellow, EO2; green, EO3; blue, EK1; brown, EK2; purple, EK3; dark grey, TO1; blue, TO2; pink, TK1; green, TK2; pink, TK3; orange, Negative Control; red.

Figure 16.

Melting Curve Analysis following Hsd17b1 Gene Amplification using qRT-PCR.

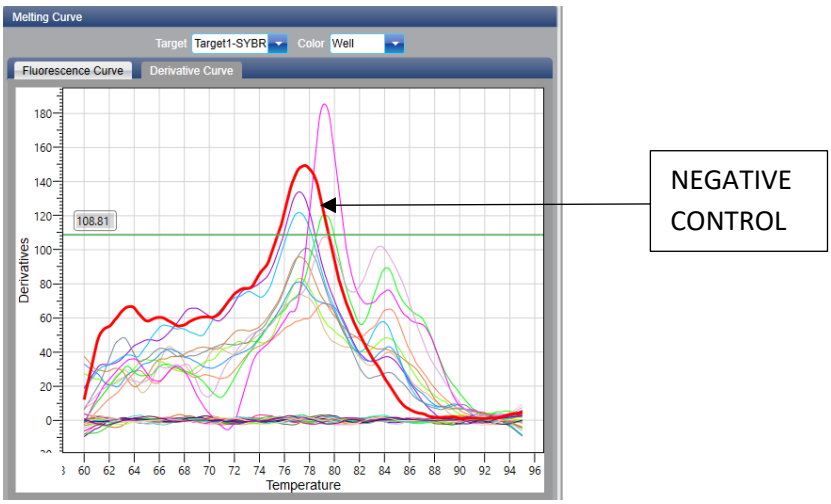

Note. A black arrow represents a negative control. The melting curve analysis showed that there was a different Tm point between the negative control (primer dimer) and the amplified product obtained from both epididymal and testicular samples of obese and control groups of rats.

Figure 17.

The Bar Chart Showing the Hsd17b1 Gene Expression Level in Rat Samples

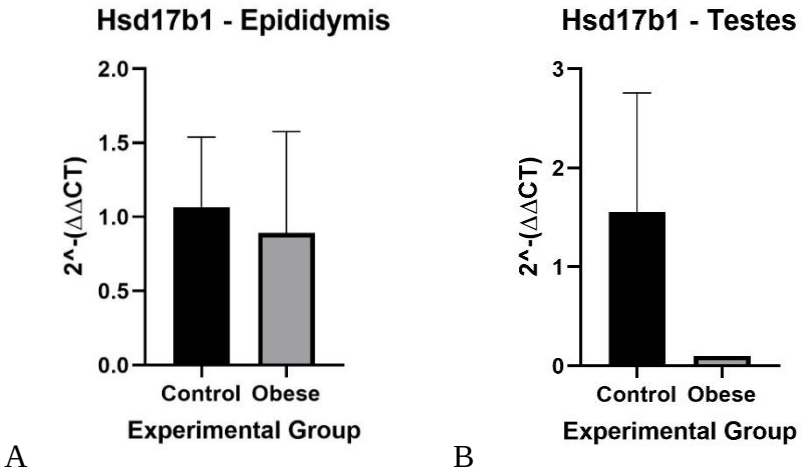

A B

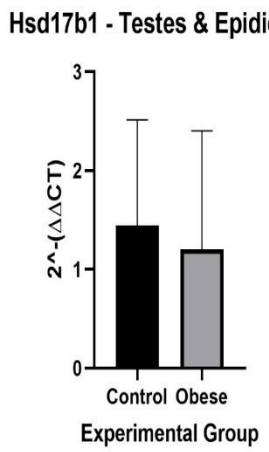

C

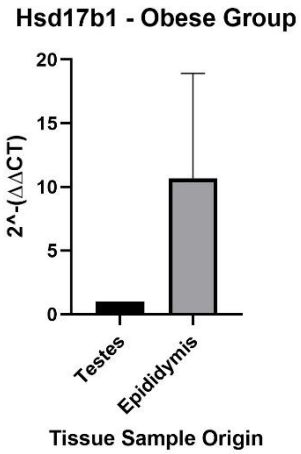

D

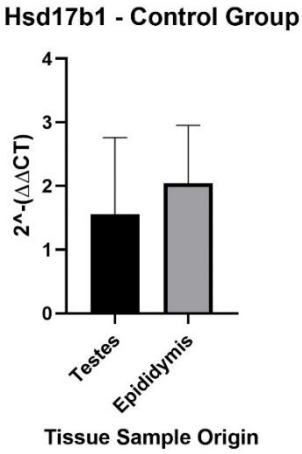

E

Note. A- The level of *Hsd17b1* gene expression was compared in rat epididymal samples obtained from control and obese rats ($p>0.05$) B- The level of *Hsd17b1* gene expression was compared in rat testicular samples obtained from control and obese rats ($p>0.05$) C- The level of *Hsd17b1* gene expression was compared in rat epidydimal and testicular samples obtained from control and obese groups rats ($p>0.05$) D- The level of *Hsd17b1* gene expression was compared in rat epidydimal and testicular samples obtained from obese groups of rats ($p>0.05$) E- The level of *Hsd17b1* gene expression was compared in rat epidydimal and testicular samples obtained from control rats groups ($p>0.05$)

All investigated gene expression levels showed no statistically significant differences when comparing among the groups. Therefore, further statistical analysis using the Kolmogorov-Smirnov test was performed. The outcome of the Kolmogorov-Smirnov statistical analysis showed a significant difference ($p<0.05$), indicating a non-normal distribution (Table 3). Moreover, a non-parametric Kruscal-

Wallis test was conducted. Nevertheless, the result indicated that the expression levels for the investigated genes between different groups were not significant ($p>0.05$) (Table 4).

Table 3.

Kolmogorov-Smirnov analysis.

Tests of Normality[a,c]				
	TK3	Kolmogorov-Smirnov[b]		
		Statistic	df	Sig.
Genenames1	25.5	.260	2	.
a. There are no valid cases for Genenames1 when TK3 = 25.100. Statistics cannot be computed for this level.				
b. Lilliefors Significance Correction				
c. Genenames1 is constant when TK3 = 26.2. It has been omitted.				

Note. Kolmogorov-Smirnov was performed for further statistical analysis. No significant levels of gene expression were observed among different groups.

Table 4.

Kruskal Wallis statistical analysis.

Kruskal Wallis testsonuç:

Test Statistics[a,b]

	EO1	EO2	EO3	EK1	EK2	EK3	TO1	TO2	TK1	TK2	TK3	NEGATİVE
Chi-Square	2.000	3.000	2.000	3.000	3.000	3.000	3.000	3.000	3.000	3.000	3.000	3.000
df	2	3	2	3	3	3	3	3	3	3	3	3
Asymp. Sig.	.368	.392	.368	.392	.392	.392	.392	.392	.392	.392	.392	.392

a. Kruskal Wallis Test

b. Grouping Variable: Genenames1

Note. Kruskal Wallis statistical analysis was performed for further statistical analysis after Kolmogorov-Smirnov analysis. No significant levels of gene expression were observed among different groups.

CHAPTER V

Discussion

In this study, a total of 11 rats, except for the *Hsd3b2* gene expression analysis, were used to investigate the level of steroidogenesis-associated gene expression; i.e. *Cyp11a1, Cyp17a1, Hsd3b2* and *Hsd17b1*. The association of gene expression levels between the obese and non-obese rats was studied in different samples obtained from the testis and epididymis. *Cyp11a1* and *Cyp17a1* genes were shown to be expressed in the testicular samples of obese and control group of rats. However, the expression of both *Cyp11a1* and *Cyp17a1* genes did not show any statistically significant difference between the obese and control groups. *Hsd3b2* and *Hsd17b1* genes were expressed in the samples of testicular and epididymal samples of obese and control group of rats. *Hsd3b2,* and *Hsd17b1* genes did not show any statistically significant difference in the testicular and epididymal samples obtained from obese and non-obese control groups of rats. Therefore, further statistical analysis of Kolmogorov- Smirnov was applied. Kolmogorov-Smirnov statistical analysis showed a p-value (Sig.) <0.05, indicating a non-normal distribution. Sample size was limited, and there were more than three groups; therefore, non-parametric Kruskal Wallis statistical analysis was performed showing that the results were non-significant for all studied genes.

Previously published studies showed that *Cyp11a1* is expressed only in the testis of rats (Payne & Hales, 2004). They also reported that *CYP11A1* expression is the only site of Leydig cells in the testis of humans (Payne & Hales, 2004). This result is also supported by 'The Human Protein Atlas' where *CYP11A1* was reported to be expressed in the testis (Uhlén et al., 2015). Despite this, previous studies reported that *CYP11A1* was found in all steroidogenic tissues (Sanderson, 2006). The current study supports the previous reports where *Cyp11a1* was not expressed in the samples obtained from the epididymal of obese and non-obese rats. Previous studies reported significant decreases in *Cyp11a1* mRNA expression in the testes of MetS rats compared to controls ($p<0.005$) (Rahali et al., 2023). In this study, no significant impact of obesity on *Cyp11a1* transcripts was observed in the testes of obese and control groups of rats ($p>0.05$).

Previous studies have reported that *Cyp17a1* shows a higher expression level in pachytene spermatocytes and spermatogonia, with minimal expression observed in

rat germ cells and mouse spermatogonia (Culty et al., 2015). This study supported that *Cyp17a1* is expressed in the testes of rats. However, this research demonstrated that *Cyp17a1* expression in the testes is not significantly related to obesity ($p>0.05$). This suggests that *Cyp17a1* does not play a significant role in these specific pathways under the conditions tested. Interestingly, inhibition of the *CYP17A1* enzyme in the steroidogenesis pathway is known to increase levels of corticosterone and 11-Deoxycorticosterone which suppresses aldosterone and renin, leading to hypertension in patients (Flück & Pandey, 2014). Obesity is associated with hypertension, and understanding the regulatory mechanisms of *CYP17A1* could provide insights into how these conditions are interconnected.

HSD3B2 is a crucial enzyme in steroidogenesis, converting the Δ5 pathway to the Δ4 pathway in the adrenal glands and gonads (Boettcher & Flück, 2022). Although this study showed that there was no considerably difference in *Hsd3b2* expression between the control and obese groups in the epididymal and testicular tissues. Literature reports that deficiencies in *HSD3B2* result in insufficient formation of mineralocorticoids, glucocorticoids, and androgens, leading to conditions like undervirilization and disorders of sex development (DSD) in 46,XY individuals (Boettcher & Flück, 2022; Flück & Pandey, 2014, 2017). These conditions are related to the function of reproductive organs. Contrary to these reports, these findings suggest that *Hsd3b2* does not play a significant role in the steroidogenesis pathway in the testes and epididymis of rats, regardless of obesity and control group status. This contrasts with previous studies indicating that long-term exposure to a high-fat diet can decrease testosterone levels and dysregulate steroidogenic gene expression in the testis (Wagner et al., 2016).

HSD17B1 plays an essential role in the pathway of steroidogenesis, like *HSD3B2* which is required for the last step in biosynthesis of testosterone under normal conditions(Payne & Hales, 2004). This study observed no significant differences in *Hsd17b1* gene expression between the control and obese groups in testicular and epididymal samples. Studies have demonstrated that rats with metabolic syndromes caused decreased testosterone levels and reduced mRNA expression of *Hsd17β* in the testis tissues (Rahali et al., 2023). Interestingly, by Fluck et.al., published that HSD17B3 insufficiency causes disorders of sex development (Flück & Pandey, 2014). This inconsistency suggests that while *HSD17B1* and *HSD3B2* are essential for steroidogenesis, their expression and regulation may

change significantly under different conditions, especially in relation to obesity and metabolic health. Thus, this study proves to be important to form the basis of the important insights into the experiments and key role of steroidogenesis enzymes in the testes and epididymis of rats.

CHAPTER VI

Conclusion

Although *Cyp11a1, Cyp17a1, Hsd3b2,* and *Hsd17b1* are widely reported for their roles in steroidogenesis, research outcomes suggest that, under the conditions studied, their expression and regulatory mechanisms in these tissues may not be significantly affected by obesity. To conciliate these differences and acquire a more comprehensive understanding, further studies should utilize more sample analysis and consider extra factors that may affect gene expression. Furthermore, investigations of these enzymes in diverse physiological and pathological conditions explain their roles and interactions within the steroidogenesis pathway.

Recommendations

To reconcile the findings with existing literature, it is recommended that the study should be expanded with a larger sample size and investigate other factors that may influence *Cyp11a1* and *Cyp17a1* expression. While *Hsd17b1* and *Hsd3b2* are essential for steroidogenesis, their expression and regulation may change remarkably in different conditions, especially concerning obesity and metabolic health.

Recommendations According to Findings

This study showed important insights into the *Cyp11a1, Cyp17a1, Hsd3b2*, and *Hsd17b1* gene expression in the steroidogenesis pathway in the testicular and epididymal tissues of obese and non-obese rats. However, several recommendations could further enhance the understanding of how obesity influences the steroidogenesis pathway. Using available techniques such as Western Blotting analysis that analyses the protein expression, future studies could reveal the protein expression of these genes in previously unknown sites within the steroidogenesis pathway.

Recommendations for Further Research

Further research is needed to focus on the long-term effects of obesity on steroidogenesis using animal models. It is essential to investigate how hormonal changes induced by obesity might influence steroidogenesis over time, particularly within the HPG-axis. Moreover, investigating the interaction between obesity and

endocrine factors, such as insulin resistance, and inflammatory cytokines on steroidogenic gene expression could provide a more comprehensive understanding. Indeed, further studies could also include protein expression analysis, along with gene expression, to assess the functional results of these changes. Finally, investigating genetic and epigenetic factors that may affect steroidogenesis in obesity would be important.

References

Belleannée, C., Thimon, V., & Sullivan, R. (2012). Region-specific gene expression in the epididymis. In *Cell and Tissue Research* (Vol. 349, Issue 3, pp. 717–731). https://doi.org/10.1007/s00441-012-1381-0

Ben Maamar, M., Nilsson, E. E., & Skinner, M. K. (2021). Epigenetic transgenerational inheritance, gametogenesis and germline development†. *Biology of Reproduction*, *105*(3), 570–592. https://doi.org/10.1093/biolre/ioab085

Boettcher, C., & Flück, C. E. (2022). Rare forms of genetic steroidogenic defects affecting the gonads and adrenals. In *Best Practice and Research: Clinical Endocrinology and Metabolism* (Vol. 36, Issue 1). Bailliere Tindall Ltd. https://doi.org/10.1016/j.beem.2021.101593

Craig, J. R., Jenkins, T. G., Carrell, D. T., & Hotaling, J. M. (2017). Obesity, male infertility, and the sperm epigenome. In *Fertility and Sterility* (Vol. 107, Issue 4, pp. 848–859). Elsevier Inc. https://doi.org/10.1016/j.fertnstert.2017.02.115

Culty, M., Liu, Y., Manku, G., Chan, W. Y., & Papadopoulos, V. (2015). Expression of steroidogenesis-related genes in murine male germ cells. *Steroids*, *103*, 105–114. https://doi.org/10.1016/j.steroids.2015.08.011

Davidson, L. M., Millar, K., Jones, C., Fatum, M., & Coward, K. (2015). Deleterious effects of obesity upon the hormonal and molecular mechanisms controlling spermatogenesis and male fertility. In *Human Fertility* (Vol. 18, Issue 3, pp. 184–193). Taylor and Francis Ltd. https://doi.org/10.3109/14647273.2015.1070438

Fang, F., Iaquinta, P. J., Xia, N., Liu, L., Diao, L., & Reijo Pera, R. A. (2022a). Transcriptional control of human gametogenesis. In *Human Reproduction Update* (Vol. 28, Issue 3, pp. 313–345). Oxford University Press. https://doi.org/10.1093/humupd/dmac002

Fang, F., Iaquinta, P. J., Xia, N., Liu, L., Diao, L., & Reijo Pera, R. A. (2022b). Transcriptional control of human gametogenesis. In *Human Reproduction Update* (Vol. 28, Issue 3, pp. 313–345). Oxford University Press. https://doi.org/10.1093/humupd/dmac002

Flück, C. E., & Pandey, A. V. (2014). Steroidogenesis of the testis - new genes and pathways. *Annales d'Endocrinologie*, *75*(2), 40–47. https://doi.org/10.1016/j.ando.2014.03.002

Flück, C. E., & Pandey, A. V. (2017). Testicular Steroidogenesis. In *Endocrinology (Switzerland)* (pp. 343–371). Springer Science and Business Media Deutschland GmbH. https://doi.org/10.1007/978-3-319-44441-3_10

Herbert, M., Kalleas, D., Cooney, D., Lamb, M., & Lister, L. (2015a). Meiosis and maternal aging: Insights from aneuploid oocytes and trisomy births. *Cold Spring Harbor Perspectives in Biology*, *7*(4). https://doi.org/10.1101/cshperspect.a017970

Herbert, M., Kalleas, D., Cooney, D., Lamb, M., & Lister, L. (2015b). Meiosis and maternal aging: Insights from aneuploid oocytes and trisomy births. *Cold Spring Harbor Perspectives in Biology*, *7*(4). https://doi.org/10.1101/cshperspect.a017970

Kahn, B. E., & Brannigan, R. E. (2017). Obesity and male infertility. In *Current Opinion in Urology* (Vol. 27, Issue 5, pp. 441–445). Lippincott Williams and Wilkins. https://doi.org/10.1097/MOU.0000000000000417

Lambard, S., Silandre, D., Delalande, C., Denis-Galeraud, I., Bourguiba, S., & Carreau, S. (2005). Aromatase in testis: Expression and role in male reproduction. *Journal of Steroid Biochemistry and Molecular Biology*, *95*(1–5), 63–69. https://doi.org/10.1016/j.jsbmb.2005.04.020

Latchoumycandane, C., Jenardhanan, P., & Mathur, P. P. (2018). Environmental impact on gametogenesis and embryogenesis: An overview. In *Encyclopedia of Reproduction* (pp. 446–451). Elsevier. https://doi.org/10.1016/B978-0-12-801238-3.64513-0

MacLennan, M., Crichton, J. H., Playfoot, C. J., & Adams, I. R. (2015a). Oocyte development, meiosis and aneuploidy. In *Seminars in Cell and Developmental Biology* (Vol. 45, pp. 68–76). Academic Press. https://doi.org/10.1016/j.semcdb.2015.10.005

MacLennan, M., Crichton, J. H., Playfoot, C. J., & Adams, I. R. (2015b). Oocyte development, meiosis and aneuploidy. In *Seminars in Cell and Developmental Biology* (Vol. 45, pp. 68–76). Academic Press. https://doi.org/10.1016/j.semcdb.2015.10.005

Mahendroo, M., Wilson, J. D., Richardson, J. A., & Auchus, R. J. (2004). Steroid 5α-reductase 1 promotes 5α-androstane-3α, 17β-diol synthesis in immature mouse testes by two pathways. *Molecular and Cellular Endocrinology*, *222*(1–2), 113–120. https://doi.org/10.1016/j.mce.2004.04.009

Maine, E. M. (2013a). Gametogenesis. In *Brenner's Encyclopedia of Genetics: Second Edition* (pp. 154–156). Elsevier Inc. https://doi.org/10.1016/B978-0-12-374984-0.00575-1

Maine, E. M. (2013b). Gametogenesis. In *Brenner's Encyclopedia of Genetics: Second Edition* (pp. 154–156). Elsevier Inc. https://doi.org/10.1016/B978-0-12-374984-0.00575-1

Marques, B., Matos, R., & Martinho, R. G. (2018). Regulation of the oocyte epigenome during prophase i arrest. In *Encyclopedia of Reproduction* (pp. 218–224). Elsevier. https://doi.org/10.1016/B978-0-12-801238-3.64457-4

Miller, W. L. (2017). Steroidogenesis: Unanswered Questions. In *Trends in Endocrinology and Metabolism* (Vol. 28, Issue 11, pp. 771–793). Elsevier Inc. https://doi.org/10.1016/j.tem.2017.09.002

Payne, A. H., & Hales, D. B. (2004). Overview of steroidogenic enzymes in the pathway from cholesterol to active steroid hormones. In *Endocrine Reviews* (Vol. 25, Issue 6, pp. 947–970). https://doi.org/10.1210/er.2003-0030

Penzias, A., Azziz, R., Bendikson, K., Falcone, T., Hansen, K., Hill, M., Jindal, S., Kalra, S., Mersereau, J., Reindollar, R., Shannon, C. N., Steiner, A., Tanrikut, C., Taylor, H., & Yauger, B. (2021). Obesity and reproduction: a committee opinion. *Fertility and Sterility*, *116*(5), 1266–1285. https://doi.org/10.1016/j.fertnstert.2021.08.018

Raad, G., Hazzouri, M., Bottini, S., Trabucchi, M., Azoury, J., & Grandjean, V. (2017). Paternal obesity: How bad is it for sperm quality and progeny health? In *Basic and Clinical Andrology* (Vol. 27, Issue 1). BioMed Central Ltd. https://doi.org/10.1186/s12610-017-0064-9

Rahali, D., Dallagi, Y., Hupkens, E., Veegh, G., Mc Entee, K., Asmi, M. El, El Fazaa, S., & El Golli, N. (2023). Spermatogenesis and steroidogenesis disruption in a model of metabolic syndrome rats. *Archives of Physiology and Biochemistry*, *129*(1), 222–232. https://doi.org/10.1080/13813455.2020.1812665

Roelofs, M. J. E. (2016). *Steroidogenesis in vitro: towards relevant models for endocrine disruptor screening*. http://www.proefschrift-aio.nl

Ruiz-Valderrama, L., Posadas-Rodríguez, J., Bonilla-Jaime, H., Tarragó-Castellanos, M. del R., González-Márquez, H., Arrieta-Cruz, I., González-Núñez, L., Salame-Méndez, A., Rodríguez-Tobón, A., Morales-Méndez, J. G., & Arenas-Riós, E. (2022). Sperm Dysfunction in the Testes and Epididymides due to Overweight and Obesity Is Not Caused by Oxidative Stress. *International Journal of Endocrinology*, *2022*. https://doi.org/10.1155/2022/3734572

Sanderson, J. T. (2006). The steroid hormone biosynthesis pathway as a target for endocrine-disrupting chemicals. In *Toxicological Sciences* (Vol. 94, Issue 1, pp. 3–21). https://doi.org/10.1093/toxsci/kfl051

Scott, H. M., Mason, J. I., & Sharpe, R. M. (2009). Steroidogenesis in the fetal testis and its susceptibility to disruption by exogenous compounds. In *Endocrine Reviews* (Vol. 30, Issue 7, pp. 883–925). https://doi.org/10.1210/er.2009-0016

Shukla, K. K., Chambial, S., Dwivedi, S., Misra, S., & Sharma, P. (2014). Recent scenario of obesity and male fertility. In *Andrology* (Vol. 2, Issue 6, pp. 809–818). Blackwell Publishing Ltd. https://doi.org/10.1111/andr.270

Tang, W. W. C., Kobayashi, T., Irie, N., Dietmann, S., & Surani, M. A. (2016). Specification and epigenetic programming of the human germ line. In *Nature Reviews Genetics* (Vol. 17, Issue 10, pp. 585–600). Nature Publishing Group. https://doi.org/10.1038/nrg.2016.88

Tremblay, J. J. (2015). Molecular regulation of steroidogenesis in endocrine Leydig cells. *Steroids*, *103*, 3–10. https://doi.org/10.1016/j.steroids.2015.08.001

Uhlén, M., Fagerberg, L., Hallström, B. M., Lindskog, C., Oksvold, P., Mardinoglu, A., Sivertsson, Å., Kampf, C., Sjöstedt, E., Asplund, A., Olsson, I. M., Edlund, K., Lundberg, E., Navani, S., Szigyarto, C. A. K., Odeberg, J., Djureinovic, D., Takanen, J. O., Hober, S., … Pontén, F. (2015). Tissue-based map of the human proteome. *Science*, *347*(6220). https://doi.org/10.1126/science.1260419

Van, L. T. (2013). Assessment of steroidogenesis and steroidogenic enzyme functions. In *Journal of Steroid Biochemistry and Molecular Biology* (Vol. 137, pp. 176–182). https://doi.org/10.1016/j.jsbmb.2013.05.017

Wagner, I. V., Klöting, N., Atanassova, N., Savchuk, I., Spröte, C., Kiess, W., Söder, O., & Svechnikov, K. (2016). Prepubertal onset of obesity negatively impacts on testicular steroidogenesis in rats. *Molecular and Cellular Endocrinology*, *437*, 154–162. https://doi.org/10.1016/j.mce.2016.08.027

Wang, Y., Chen, F., Ye, L., Zirkin, B., & Chen, H. (2017). Steroidogenesis in leydig cells: Effects of aging and environmental factors. In *Reproduction* (Vol. 154, Issue 4, pp. R111–R122). BioScientifica Ltd. https://doi.org/10.1530/REP-17-0064

WHO. (2022, March 1). *Obesity and overweight*. https://www.who.int/news-room/fact-sheets/detail/obesity-and-overweight

Yi, X., Gao, H., Chen, D., Tang, D., Huang, W., Li, T., Ma, T., & Chang, B. (2017). Effects of obesity and exercise on testicular leptin signal transduction and testosterone biosynthesis in male mice. *American Journal of Physiology - Regulatory Integrative and Comparative Physiology*, *312*(4), R501–R510. https://doi.org/10.1152/ajpregu.00405.2016

APPENDICES

Appendix

Ethical Approval

T.C.
Manisa Celal Bayar Üniversitesi
Hayvan Deneyleri Yerel Etik Kurulu

KARAR TARİH / NO	16/ 04 / 2020 / 77.637.435			
ARAŞTIRMANIN ADI	Sistein- Zengin Sekretuar Proteinleri (Crısps) Deneysel Obez Erkek Sıçanlarda İnfertilite İle İlişkisi			
SORUMLU ARAŞTIRMACI	Prof. Dr. H. Seda VATANSEVER - Histoloji ve Embriyoloji Anabilim Dalı			
ARAŞTIRMA EKİBİ	Souleymane ADALE IDI			
ARAŞTIRMANIN NİTELİĞİ	**UZMANLIK TEZİ** ☐	**YÜKSEK LİSANS~~-DOKTORA TEZİ~~** ☒	**AKADEMİK AMAÇLI** ☐	Eğitim ☐
DEĞERLENDİRİLEN BELGELER	19 / 03 / 2020 / Tarih ve 12165 sayılı; araştırma dosyası			
KARAR BİLGİLERİ	Araştırma dosyası incelenmiş, bilimsel ve etik açıdan **UYGUN** olduğuna oy birliği ile karar verilmiştir.			

Unvanı/Adı/Soyadı		Araştırma İle İlişkisi Olan Üye	Toplantıya Katılmayan Üye	Unvanı /Adı /Soyadı		Araştırma İle İlişkisi Olan Üye	Toplantıya Katılmayan Üye
Prof. Dr. Ercüment ÖLMEZ		☐	☐	Prof. Dr. Gökhan TEMELTAŞ		☐	☐
Prof. Dr. İsmet TOPÇU Anestezi ve Reanimasyon AD		☐	☐	Prof. Dr. Özge YILMAZ Çocuk Hastalıkları AD.		☐	☐
Prof. Dr. Ertuğrul TATLISUMAK Anatomi AD	-------	☐	☒	Dr. Öğr. Üyesi Fulya OCAK – Veteriner Hekim		☐	☐
Prof. Dr. Kıvanç GÜNHAN (DEHAM MD)		☐	☐	Saime ÖZKARA Sivil Toplum Üyesi		☐	☐
Dr. Öğr. Üyesi Selim ALTAN Tıp Tarihi ve Etik AD		☐	☐	Levent ÖDEMİŞ Sivil Üye	———	☐	☒

Etik Kurulumuzun kararı yukarda belirtilmiştir. Araştırma Başvuru Formunun Taahhütname kısmında belirtilmiş olan hususların dikkate alınarak istenilen bilgilerin Etik Kurulumuza zamanında iletilmesi konusunda bilgilerinizi ve gereğini rica ederim.

Ercüment ÖLMEZ
Başkan

CV

ÖZGEÇMİŞ VE ESERLER LİSTESİ

ÖZGEÇMİŞ

Adı ve Soyadı: Selin Temi

Doğum Tarihi: 21.10.1999

Doğum Yeri: Lefkosa

Akademik Unvanı: Molekuler Biyolog

İş Telefonu: --

Cep Telefonu: +905428805089

İş Adresi: Şht. Ecvet Yusuf Caddesi 44A-44D Yenişehir - Lefkoşa / KKTC

E-postası: temiselin@gmail.com

Bildiği Yabancı Diller (Puan ve Yılı):

Aldığı Sertifikalar: Advance Course in Clinical Embryology, University of Athens

Uzmanlık Alanı:

Derece	Bölüm/Program	Üniversite	Yıl
Lisans	Molecular Biology and Genetics	Yakin Dogu Universitesi	2017-2021
Y. Lisans	Medical Biology and Genetics	Yakin Dogu Universitesi	2021-
Doktora			
Doç. / Prof.			

Yüksek Lisans Tez Başlığı (özeti ekte) ve Tez Danışman(lar)ı: Expression of Genes Involved in Steroidogenesis Pathway From Testicular and Epididymal Samples of Obese and Non-Obese Rats - Prof. Dr. Pınar TULAY, Dr. Gulten TUNCEL and Dr. Hakan AYTACOGLU

Selin Temi Thesis

ORIGINALITY REPORT

14%	8%	12%	%
SIMILARITY INDEX	INTERNET SOURCES	PUBLICATIONS	STUDENT PAPERS

PRIMARY SOURCES

1	Christa E. Flück, Amit V. Pandey. "Steroidogenesis of the testis–new genes and pathways", Annales d'Endocrinologie, 2014 Publication	1%
2	link.springer.com Internet Source	1%
3	Anita H. Payne, Dale B. Hales. "Overview of Steroidogenic Enzymes in the Pathway from Cholesterol to Active Steroid Hormones", Endocrine Reviews, 2004 Publication	1%
4	boris.unibe.ch Internet Source	1%
5	Martine Culty, Ying Liu, Gurpreet Manku, Wai-Yee Chan, Vassilios Papadopoulos. "Expression of steroidogenesis-related genes in murine male germ cells", Steroids, 2015 Publication	1%
6	S. Lambard, D. Silandre, C. Delalande, I. Denis-Galeraud, S. Bourguiba, S. Carreau. "Aromatase in testis: Expression and role in male reproduction", The Journal of Steroid Biochemistry and Molecular Biology, 2005 Publication	<1%
7	Jeong Yoon Lee, Hyo-Kyoung Choi, Kyung-Chul Choi, Mina Jo, Jung-Yoon Yoo, Yoo-Hyun Lee. "The effect of Sasa borealis on improving	<1%